

**EXAMINATION OF DETERIORATION  
PROBLEMS OF ANDESITE USED IN  
AIGAI AGORA**

**A Thesis Submitted to  
the Graduate School of Engineering and Sciences of  
İzmir Institute of Technology  
in Partial Fulfillment of the Requirements for the Degree of**

**MASTER OF SCIENCE**

**in Architectural Restoration**

**by  
Fulya MURTEZAOĞLU**

**July 2009  
İZMİR**

We approve the thesis of **Fulya MURTEZAOĞLU**

---

**Prof. Dr. Hasan BÖKE**  
Supervisor

---

**Prof. Dr. Başak İPEKOĞLU**  
Committee Member

---

**Assist. Prof. Dr. Engin AKTAŞ**  
Committee Member

---

**Prof. Dr. Ersin DOĞER**  
Committee Member

---

**Prof. Dr. Zeynep MERCANGÖZ**  
Committee Member

**01 July 2009**

---

**Prof. Dr. Başak İPEKOĞLU**  
Head of the Architectural Restoration  
Department

---

**Prof. Dr. Hasan BÖKE**  
Dean of the Graduate School of  
Engineering and Science

## ACKNOWLEDGEMENTS

This thesis might not have existed without the support of many people.

First of all, I would like to express my special thanks to my supervisor Prof. Dr. Hasan Bke for his scientific support, guidance and patience throughout the study. I would never learned the things I have during this study without your help.

I also would like to express my gratefulness to Prof. Dr. Bařak İpekođlu for her encouragement and support in several projects during my master education. Thank you for your remarkable contributions to this thesis whenever needed.

My thanks to the jury members for their attendance at my thesis defence seminar and for their valuable suggestions to this study.

Also thanks to the research scientists of the Centre for the Materials Research of the Institute for SEM-EDS, XRD, TGA and petrographic analyses.

Studying in an archaeological site as Aigai was a different experience for me as an architect. Here, I would like to thank Prof. Dr. Ersin Dođer, who is the head of Aigai excavation team, for his hospitality and permission to prepare this thesis. Thank you for sharing your knowledge and archieve for this research.

And of course, thanks to my dear friends who worked with. Thanks to my dear friend ađlayan Deniz Kaplan for being such a good term-mate and friend like a brother. I hope we study in several projects together. Thanks to my dear friends Elif Uđurlu and Kerem řerifaki for their valuable technical help, encouragement, and neverending friendship. Studying in this lab and living in this city would not be so enjoyable and fruitful without any of you.

Finally, I am indebted to my mother Nilgn Murtezaođlu, my father Hızır Murtezaođlu and my brother Ufuk Murtezaođlu for their endless love, support and patience throughout my life. This thesis is dedicated to them.

## ABSTRACT

### EXAMINATION OF DETERIORATION PROBLEMS OF ANDESITE USED IN AIGAI AGORA

The archaeological sites should be conserved as being the documents of ancient civilizations as a part of the built cultural heritage. In this study, the deterioration problems of stone used in the construction of the agora building in the archaeological site of Aigai (Manisa/Turkey) was investigated for the aim of its conservation. For this purpose, the building was documented by photographs and drawings. The stone deteriorations were documented on the drawings and samples were collected from the deteriorated and sound parts of stones. Basic physical properties, mineralogical, chemical and microstructural characteristics of the stone samples were determined to define the causes of deteriorations. X-Ray diffraction, scanning electron microscope, polarized microscope, infrared spectroscopy and thermogravimetric analyzer were used in the analysis.

The stone used in the building is andesite which is mainly composed of andesine, albite high, anorthite, kyanite, labradorite, muscovite, microcline, mullite, orthoclase, orthoferrosilite, quartz, sanidine and tridymite minerals. The density and porosity values of sound andesite are  $2.4 \text{ g/cm}^3$  and 8 % by volume respectively. On the weathered parts of the stone, the porosity increases with degree of weathering. The depth of the weathered zone from the surface to the inner parts which was determined by SEM analysis is about 1.7 cm. On the weathered parts of stone, clay minerals and iron oxides were determined as weathering products of andesite. The existence of clays on the exterior and the interior parts of the andesite accelerates weathering by their swelling–shrinkage properties and provide suitable conditions for the biological growth. Main weathering forms observed on the stone surfaces are detachment, deposits and loss of stone materials. The progress of weathering forms depends mainly on the difference in temperature and humidity between night and day at the site. Condensation and frost occurs mostly in winter months with increasing relative humidity and decreasing temperature. Humid and rainy conditions of winter months promote the weathering of the stone.

## ÖZET

### AİGAI AGORASINDA KULLANILAN ANDEZİTİN BOZULMA SORUNLARININ İNCELENMESİ

Eski uygarlıkların belgelerini oluşturan arkeolojik alanlar, kültürel mirasın birer parçası olarak korunmalıdır. Bu çalışmada, Aigai (Manisa/Türkiye) arkeolojik alanındaki agora binasının korunması amacıyla, binanın yapımında kullanılan taşların bozulma sorunları incelenmiştir. Bu amaçla, yapı fotoğraf ve çizimler ile belgelenmiştir. Taş bozulmaları çizim üzerinde belgelenmiş ve taşların sağlam ve bozulmuş kısımlarından örnek toplanmıştır. Bozulma sebeplerinin tanımlanması için taş örneklerinin temel fiziksel, mineralojik, kimyasal ve mikroyapısal özellikleri belirlenmiştir. Analizlerde, X ışınları kırınım cihazı, taramalı elektron mikroskobu, polarize mikroskop, kızılötesi spektroskopisi ve TGA kullanılmıştır.

Yapıda kullanılan taş, temel olarak andezin, albit, anortit, kiyanit, labradorit, muskovit, mikrolin, mullit, ortoklaz, ortoferrosilit, kuvars, sanidin, tridimit minerallerinden oluşan andezittir. Sağlam andezitin yoğunluk ve gözeneklilik değerleri sırasıyla  $2.4 \text{ g/cm}^3$  ve hacim olarak % 8'dir. Taşın bozulmuş kısımlarında, bozulma derecesi ile birlikte gözeneklilik artar. SEM analizleri ile belirlenen bozulma zonunun derinliği, yüzeyden içlere doğru 1.7 cm civarındadır. Bozulmuş kısımlarda, andezitin bozulma ürünleri olan kil mineralleri ve demir oksitler belirlenmiştir. Andezitin iç ve dış kısımlarında killerin bulunması, şişme-büzülme özellikleri ve biyolojik oluşumlara uygun ortam oluşturmaları sebebiyle bozulmayı hızlandırır. Taş yüzeylerinde görülen başlıca bozulma tipleri ayrılma, tortu oluşumu ve taş malzemedeki kayıptır. Bozulma tiplerinin ilerlemesi, alanda gece-gündüz sıcaklık ve nem farklarına bağlıdır. Yoğunlaşma ve donma, düşen sıcaklık ve artan bağıl nem ile en çok kış aylarında oluşur. Kış aylarının nemli ve yağmurlu koşulları taşın bozulmasını artırmaktadır.

# TABLE OF CONTENTS

LIST OF FIGURES .....	viii
LIST OF TABLES.....	xii
CHAPTER 1. INTRODUCTION.....	1
1.1. Historical and Architectural Characteristics of Aigai Agora.....	2
1.1.1. Architectural Characteristics of Aigai Agora .....	5
1.1.2. Present Condition of Aigai Agora .....	9
1.2. Construction Technique and Materials of Aigai Agora.....	11
1.2.1. Stones Used in the Construction of Aigai Agora .....	13
1.2.2. Weathering of Andesite .....	15
1.3. Climatic Characteristics of the Site.....	17
1.4. Aim of the Study.....	21
CHAPTER 2. SITE SURVEY.....	23
2.1. Visual Analysis of Stone Weathering Observed on the Southeast Wall of Aigai Agora .....	23
2.2. Mapping of Weathering Forms Observed on the Southeast Wall of Aigai Agora .....	30
2.3. Structural Problems Observed on the Southeast Wall of Aigai Agora.....	33
CHAPTER 3. EXPERIMENTAL STUDY .....	35
3.1. Sampling .....	35
3.2. Experimental Methods.....	40
3.2.1. Determination of Basic Physical Properties of Andesite.....	40
3.2.2. Determination of Particle Size Distribution of Infill Material .....	41
3.2.3. Determination of Mineralogical and Chemical Compositions of Andesite and Infill Material.....	41
3.2.4. Determination of Microstructural and Petrographical Characteristics of Andesite.....	42

3.2.5. Determination of Weight Loss of Andesite by Thermogravimetric Analysis.....	42
3.2.6. Determination of Salt Content.....	43
CHAPTER 4. RESULTS AND DISCUSSION.....	44
4.1. Characteristics of Andesite used in the Construction of Aigai Agora .....	44
4.1.1. Basic Physical Properties of Andesite .....	44
4.1.2. Mineralogical Composition of Andesite.....	44
4.1.3. Chemical Composition of Andesite.....	45
4.1.4. Microstructural and Petrographical Characteristics of Andesite.....	46
4.1.5. Weight Loss of Andesite by Thermogravimetric Analysis .....	50
4.2. Characterization of Infill Material in the Rubble Core of the Wall.....	51
4.2.1. Particle Size Distribution of Infill Material .....	51
4.2.2. Mineralogical Composition of Soil Fraction in the Infill Material .....	53
4.2.3. Chemical Composition of Soil Fraction in the Infill Material .....	55
4.2.4. Weight Loss of Soil Fractions by Thermogravimetric Analysis.....	56
4.3. Main Causes of Weathering of Andesite .....	57
4.3.1. Effects of Climatic Conditions on the Weathering of Andesite.....	58
4.3.2. Effects of Clay Minerals on the Weathering of Andesite.....	64
4.3.3. Effects of Biological Growth on the Weathering of Andesite.....	66
4.3.4. Effect of Salt Crystallization on the Weathering of Andesite .....	68
CHAPTER 5. CONCLUSION .....	71
REFERENCES .....	73

# LIST OF FIGURES

<b><u>Figure</u></b>	<b><u>Page</u></b>
Figure 1. Location of Aigai .....	3
Figure 2. Site plan of Aigai .....	4
Figure 3. General view of Aigai Agora.....	5
Figure 4. Restitutions of Floor plans of Agora.....	6
Figure 5. Location of Macellum and Agora.....	6
Figure 6. Entrance door and window openings of the 6 <sup>th</sup> chamber.....	8
Figure 7. Restitution drawing of Agora .....	8
Figure 8. Sun-brokers on the facade of the third floor .....	9
Figure 9. Collapsed parts inside of the building.....	10
Figure 10. Photographs showing the wall in 1886 a) and in 2007 b).....	10
Figure 11. Southeast wall of Agora in 1886.....	11
Figure 12. Section of the southeast wall .....	12
Figure 13. Section of the Southeast wall showing infill material with soil and pebble stone.....	13
Figure 14. Average values of the average monthly values of ambient temperature, relative humidity and dew-point temperature between the years 1996 and 2006 .....	19
Figure 15. Average values of average monthly values of rainfall between the years 1996 and 2006 .....	19
Figure 16. Average values of the average monthly values of windspeed between the years 1996 and 2006 .....	19
Figure 17. Average values of the average monthly values of ambient temperature and relative humidity between the years 1996 and 2006; hour: 7:00 a), 14:00 b), 21:00 c).....	20
Figure 18. Average values of the average monthly frosty days between the years 1996 and 2006 .....	21
Figure 19. Relief observed on the stone surfaces of Agora .....	25
Figure 20. Relief observed on the stone surfaces of Agora .....	25
Figure 21. Back weathering observed on the stone surfaces of Agora .....	25
Figure 22. Back weathering observed on the stone surfaces of Agora .....	25



Figure 23. Break out observed on some parts of the building stones of Agora .....	26
Figure 24. Break out observed on some parts of the building stones of Agora .....	26
Figure 25. Coloration and white deposition observed on the stone surfaces of Agora .....	26
Figure 26. Microbiological colonization observed on the stone surfaces of Agora .....	26
Figure 27. Microbiological colonization observed on the stone surfaces of Agora .....	26
Figure 28. Black crust observed on the stone surfaces of Agora .....	27
Figure 29. White deposition observed on the lintels of door and window openings of Agora.....	27
Figure 30. Higher plants observed on some parts of Southeast facade of Agora .....	27
Figure 31. Higher plants observed on some parts of Southeast facade of Agora .....	27
Figure 32. Granular disintegration observed on the stones of Agora.....	28
Figure 33. Granular disintegration observed on the stones of Agora.....	28
Figure 34. Scaling observed on the stone surfaces of Agora .....	28
Figure 35. Scaling observed on the stone surfaces of Agora .....	28
Figure 36. Detachment of black crust observed on the stone surfaces of Agora .....	28
Figure 37. Detachment of black crust observed on the stone surfaces of Agora .....	28
Figure 38. Cracks a) and fissures b) observed on the stones of Agora .....	29
Figure 39. Mapping of weathering forms observed on the Southeast Facade of the building.....	32
Figure 40. Relief and traces of tooling on stone surfaces and the sound corner parts without tooling at the southeast corner of the building .....	33
Figure 41. Effect of efflorescence and granular disintegration.....	33
Figure 42. Cracks formed on the eastern corner of the building.....	34
Figure 43. Fissures formed on the lintels of door and window openings .....	34

Figure 44. Partial elevation of Agora, showing where the samples were collected.....	36
Figure 45. Collapsed building stones, showing where the andesite samples were collected (A.St.1 and A.St.2) .....	36
Figure 46. Southeast facade of the wall, showing where the andesite samples were collected (A.St.3) .....	37
Figure 47. Southeast facade of the wall, showing where the andesite samples were collected (A.St.4) .....	37
Figure 48. Rubble core, showing where infill materials were collected (A.S).....	38
Figure 49. Lintel of 7 <sup>th</sup> chamber showing where samples of efflorescence were collected (A.Eff.1).....	38
Figure 50. XRD pattern of sound andesite sample from the inner part .....	45
Figure 51. Graph a) and table b) showing the amounts of major and minor elements in unweathered andesite sample .....	46
Figure 52. BSE images of feldspar, biotite a), iron and quartz b) in the matrix of andesite sample .....	47
Figure 53. BSE image showing the amorphous phases in the composition of andesite .....	48
Figure 54. Thin section images of feldspar a), b) and biotite minerals c) in the matrix of sound andesite sample x40.....	50
Figure 55. TGA graph of the sound andesite sample from the inner part of the stone .....	51
Figure 56. Particle size distribution of aggregates of soil used as infill material in the rubble core .....	52
Figure 57. Stereo microscope images of aggregates in the soil used as infill material in the rubble core .....	53
Figure 58. XRD patterns of soil sample a) and soil fraction less than 53 $\mu\text{m}$ b).....	54
Figure 59. FT-IR graphs of soil sample a) and soil fraction less than 53 $\mu\text{m}$ b) taken from infill.....	55
Figure 60. Graph a) and table b) showing the amounts of major and minor elements in soil taken from infill .....	56
Figure 61. TGA graph of soil fraction less than 53 $\mu\text{m}$ taken from soil infill .....	57

Figure 62. Porosity change from exterior surface to sound inner parts of the stone .....	59
Figure 63. BSE image of crack formation from exterior surface a) to the sound inner parts b) of the stone .....	61
Figure 64. XRD patterns of weathered andesite samples taken from the exterior surface a) and inner crack surface of the stone b) .....	63
Figure 65. FT-IR spectrum of samples taken from inner crack surface of the stone .....	64
Figure 66 Elemental compositions of unweathered and weathered stone samples.....	64
Figure 67. Scaling as a result of clay formation inside of the stone .....	65
Figure 68. SE images of clay deposition on the exterior a) and inner crack surfaces with microbiological growth b) .....	65
Figure 69. Lichen colonization on the upper parts of the wall.....	66
Figure 70. Lichen colonization on the northeast facade of the building.....	67
Figure 71. Optic microscope image a), SE image b), EDX spectrum c) and chemical composition d) of lichens taken from the exterior surface of andesite .....	67
Figure 72. Soluble salt content of unweathered and weathered andesite and infill material.....	68
Figure 73. Efflorescence on the surfaces of vertical and horizontal stone blocks defining the entrance to the 7th interior chamber.....	69
Figure 74. BSE images a), b), EDX spectrum c) and chemical composition d) of efflorescence taken from the surface of the stone of horizontal lintel, A.Eff.1 .....	69
Figure 75. FT-IR spectrum of efflorescence taken from the surface of the stone of the horizontal lintelhe surface of the stone of the horizontal lintel.....	70

## LIST OF TABLES

<b><u>Table</u></b>	<b><u>Page</u></b>
Table 1. The observed weathering forms of stone on the Southeast wall of Agora .....	24
Table 2. Samples collected from the site .....	39

# CHAPTER 1

## INTRODUCTION

Archaeological sites, which have existed for thousand years, are important parts of the world's cultural heritage which documents the lives of ancient civilizations. The findings in the archaeological sites such as ruins of buildings, coins, ceramic jars, bones, etc. are witnesses of historical development of the ancient cities.

Archaeological sites were first taken into consideration in an international meeting based on the conservation of historic monuments and archaeological sites named as Madrid Conference in 1904. Since then, the conservation approaches and techniques which will be applied in the conservation of these sites have been discussed and developed.

Archaeological sites give information about the city including its socio-cultural classes, administrative body, economy, army, social activities, settlement relationships with the surrounding civilizations in the same period, settlement organization, architectural characteristics, tectonic, structural system and material usage with their problems and potentials. Hence, these sites should be conserved beginning with a proper conservation approach, management and techniques, and the conservation should be carried out in a multidisciplinary way with contributions of several experts from different disciplines such as archaeology, architecture, engineering, chemistry, biology etc (ICOMOS Charter 2009).

The main aim of the studies which will be held in historical sites must be the conservation of them for future generations with all their authentic characteristics with respect to their original materials and techniques. In this case, documentation is one of the crucial phases for the conservation of a historical building. While documenting the architectural characteristic of the building, structural characteristics and material use should be investigated. In order to decipher the structural characteristics of the building, this phase of the conservation work should include the investigation of material

characteristics, deterioration problems and their causes considering the climatic conditions of the site (Schaffer 1932).

In this study, the characteristics and the weathering problems of stones used in the construction of the agora in the archaeological site of Aigai have been investigated considering the climatic conditions of the site.

In this chapter, the historical and architectural characteristics of Aigai and the agora, its present condition, construction technique and characteristics of the building stone used in the case study building will be introduced considering the previous studies.

## **1.1. Historical and Architectural Characteristics of Aigai Agora**

Aigai, which is also known as Nemrutkale (Bohn and Schuchhardt 1889) on the River of Kocayay, is an archaeological site located on Gün Mountain 360 meters from sea level. It is approximately 2 km from Kösel village on the west of Manisa. The settlement was studied by MM. Ramsay, D. Baltazzi, and M. Reinach in 1881, by M. Clerc in 1882 (Frothingham 1886). It was then studied in 1885 by R. Bohn and C. Schuchhardt, two members of the Pergamon excavation team whose aim was to gain information concerning Aigai to contribute to the studies in the excavation of Pergamon for a comparative study (Bohn and Schuchhardt 1889). The latest studies have been carried out in Aigai starting in 2004 by Aegean University through the leadership of Prof. Dr. Ersin Doğer. The study has been carried out in different fields of the area such as the main roads coming through the necropolis, bouleuterion and some parts of the agora since 2004.

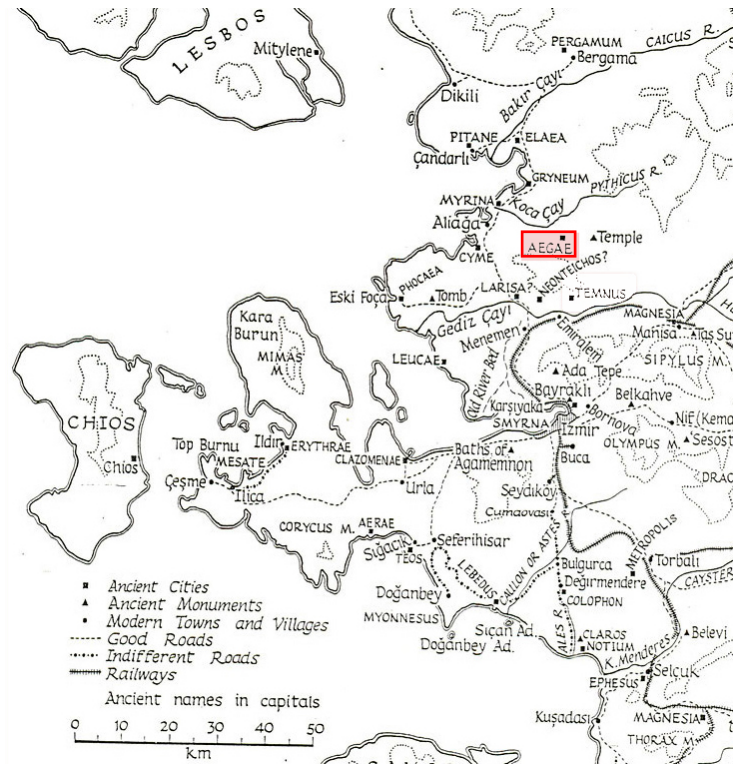


Figure 1. Location of Aigai  
(Source: Roma Tre University 2008)

The settlement, which was used in different time periods beginning with the archaic period (Doğer 2007), was one of the 12 independent Aiolis cities in the Aegean zone ahead of Kyme in the Hellenistic Period (Herodotus 1991). Being settled away from the sea like Temnus (another Aiolic city), Aigai was different from other Aiolis cities (Figure 1). According to Schuchhardt, although there was not any industrial or commercial network around it, the location of the settlement was important because of being an outpost for any dangers coming from the mountains to the coastal settlements (Bohn and Schuchhardt 1889). Because of its strength, Aigai was not affected from the Persian irruptions in the end of the 6th and the beginning of the 5th centuries B.C. (Ramsay 1881). However, it suffered a lot during the wars in the 3rd century B.C. between Attalos I and Akhaios. Finally, the city was in the hegemony of Pergamon in 218 B.C. Aigai was also affected from the wars between Attalus I from the Kingdom of Pergamon and Prusias II from Bithynia. In this period and after, the city was always alined with Pergamon. Bohn points out that this may be the reason for the similarities in the settlement organization and the use of the topography between Pergamon and Aigai such as building terraces on a sloped area. In 46 B.C., Publius Servilius Isauricus, who

was the proconsul of Asia Minor, erected and restored several buildings of the settlement. The Roman ruins in the Southern part are thought to have been built in this period (Bohn and Schuchhardt 1889). Tacitus mentions an earthquake that damaged the 12 Aeolis cities in 17 A.D. (Tacitus 2009). Aigai was one of them and the ruined buildings in the settlement were restored by the order of Emperor Tiberius in 34-35 A.D. (Doğer 2007). The information that the city was used by the Byzantines was deciphered from the Byzantine building additions and ruins in the site. After the city was abandoned, the cut-stones of the buildings were used by the people who lived in the surroundings in the construction of their own houses. At present, the main building ruins, which are determined with their locations in the settlement, are bouleuterion, theatre, small shops on the main pathway in front of the bouleuterion, bath, stadion, agora, macellum, temples and cisterns in different levels and places (Figure 2).



A: Northern Bath, B: Demirkapı, C: Yeni Kapı, D: Bouleuterion, E: Agora, F: Acropolis, G: Theatre, H: Stadion

Figure 2. Site plan of Aigai  
(Source: The archives of Aigai excavations 2005, Bohn and Schuchhardt 1889)



### 1.1.1. Architectural Characteristics of Aigai Agora

Agora, which was a gathering space of the citizens, was firstly settled on a large, flat area close to the acropolis. It was the most important part of the settlement in the archaic period. By the Hellenistic period, agora became more than an addition to the city and constituted the city centre. When the agora complex completed its evolution in the 3rd century B.C., this area was defined by some building masses as bouleuterion, stoa surrounding the agora, market hall, protaneion and temples. The most important building mass was the stoa, a semi-open colonnaded area, which defined the shape of the agora as well.

Stoa firstly appeared with the need of a shelter to protect people from sun and rain in the Mediterranean cities. In addition, it was also used for several purposes such as political, cultural and commercial activities. In some of the Hellenistic examples, there are two agora spaces in the city; one is the upper agora where political and governmental activities were carried out, and the lower agora known as market hall which was used for commercial activities (Wycherley 1993). In this case study, the studied building (Figure 3), known as agora is thought to be both, where it provides small shops on the ground floor, a large storage area on the first floor considering the restitution drawings of Bohn (Figure 4), and a stoa on the second floor defining the agora square at southeast of the bouleuterion (Bohn and Schuchhardt 1889).



Figure 3. General view of Aigai Agora

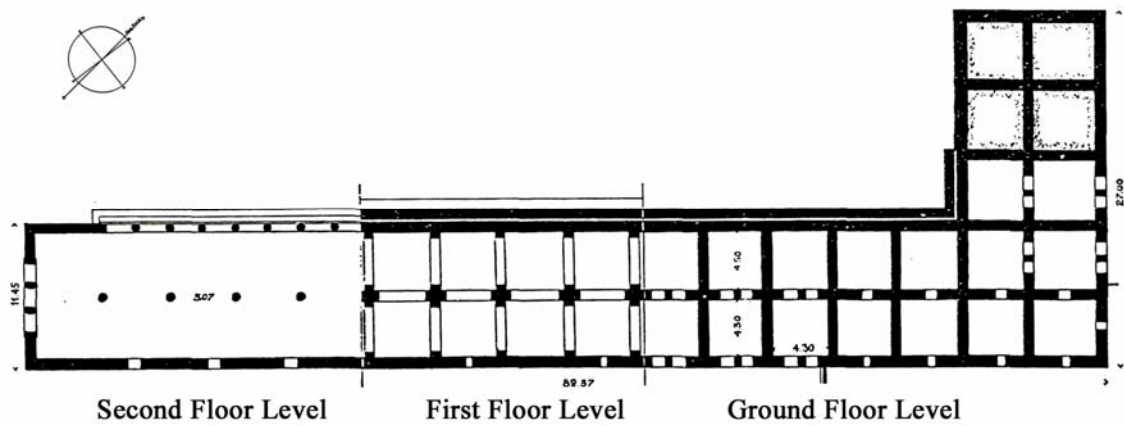


Figure 4. Restitutions of Floor plans of Agora  
(Source: Bohn and Schuchhardt 1889)

The studied agora is a three-storied masonry building dating to Hellenistic period. It is located on the southeast of the city in the north-south direction. The main pathway to the city goes along the northwest of the building to the Agora from a gateway, Yenikapı. There is also another pathway at its southeast which comes from another gateway of the city, Demirkapı. To the southeast of this building, there is a trace of a circular planned building or space (8.50 m in diameter), which is thought to be a *macellum* where meat and fishes were sold (Figure 5) (Doğer 2006, Doğer 2007).

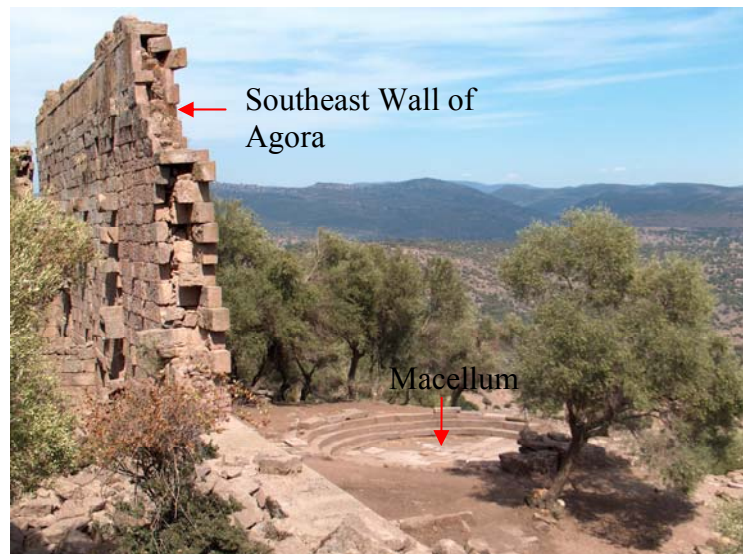


Figure 5. Location of Macellum and Agora  
(Source: The archives of Aigai excavations 2005)

Agora is located on a sloped site. Two of its stories are below the artificial terrace level supporting the stoa on the third floor at its northwest which is similar in the stoas of Assos and Alinda (Dinsmoor 1989). The Aigai Agora is an L-shape planned building with the dimensions of 82.37 m  $\times$  27.00 m in two wings. It forms the upper agora with a stoa on the third floor level.

On the ground floor, there are 38 chambers which form two rows of similar chambers. The outer sixteen chambers (approximately 4.30 m  $\times$  4.30 m in plan) are adjacent to the southeast wall of agora. The twelve of these chambers may be entered directly from the outside at the southeast. Each of them has one entrance door opening (app. 1.00 m in width and 2.05 m in height) and one window opening (1.00 m in width and height) each shrinking towards the top (Figure 6). The inner chambers, which are similar in size and shape, are located behind the division walls (2.20 m height and 0.78 m width) at the northwest row. Also, each of inner twelve chambers with similar dimensions (approximately 4.30 m  $\times$  4.50 m) has similar door and window openings on the division walls between the two chambers. It may be proposed that they have the similar spatial characteristics with the ones at south except having direct sunlight and a direct entrance from the outside.

The entrance to the first floor was provided from the northwest door. The restitution drawings show that this was an area without a division wall carried by the arches and columns as it is also understood from the traces coming from the building itself (Figure 7) (Bohn and Schuchhardt 1889). At the level of this storey on the southeast facade, there were smaller openings with sun-brokers (Figure 8). As Ramsay states, these openings were on top to every two doors beneath (Ramsay 1881). However, only two of them exist at present.

The second floor was a semi-opened colonnaded area, known as stoa, on the southeast of agora.



Figure 6. Entrance door and window openings of the 6<sup>th</sup> chamber

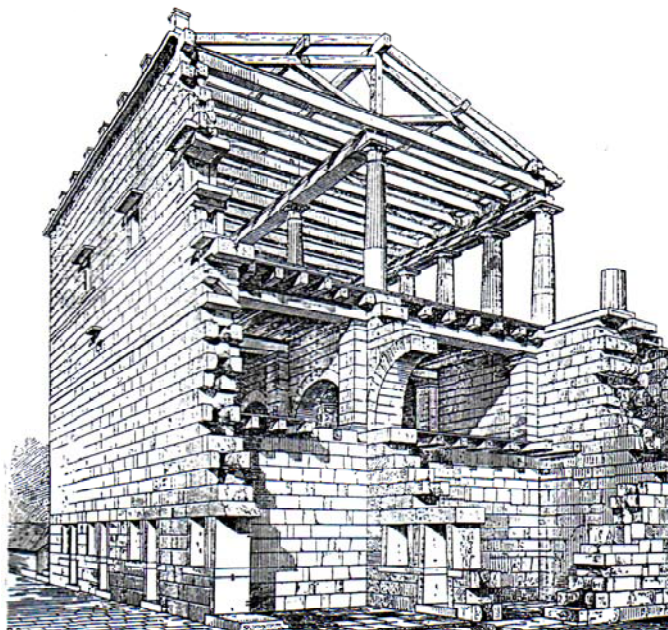


Figure 7. Restitution drawing of Agora  
(Source: Bohn and Schuchhardt 1889)



Figure 8. Sun-breakers on the facade of the third floor

### **1.1.2. Present Condition of Aigai Agora**

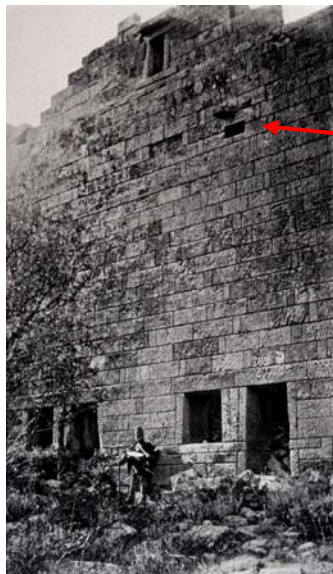
The ancient city Aigai is located in a suburban area away from the city centre at present. There is no transportation by vehicles to the ancient city. So, the city was not extremely destroyed. However, people living in the close-by surroundings used the building stones of the monuments in the construction of their own buildings. The stones of agora are observed in the houses of the people living in Köseler village.

The excavation team excavated one chamber on the ground floor of agora during the summers of 2005 and 2006.

The upper parts of the structure have collapsed and are laid in the chambers at the ground floor causing compression on the southeast wall of the building (Figure 9). In the pictures of the agora dating to 1886 (Bohn and Schuchhardt 1889), the first and second floor and the roof do not exist as at present. However, the southeast wall of the structure was in better condition than now considering the fallen building stones (Figure 10 and Figure 11). The material deteriorations of the building are defined as loss of stone material, discoloration and deposit, and detachment in general (Fitzner 2001).



Figure 9. Collapsed parts inside of the building



a)



b)

Figure 10. Photographs showing the wall in 1886 a) and in 2007 b) (Source: a) Bohn and Schuchhardt 1889)



Figure 11. Southeast wall of Agora in 1886  
(Source: Bohn and Schuchhardt 1889)

## 1.2. Construction Technique and Materials of Aigai Agora

The Aigai agora is a three-storied stone masonry building. Cut-stone andesite, soil and stone pieces are used as building materials in this load-bearing structure.

There are three parts in the sections of the walls: outer facing, rubble core and inner facing (Figure 12). In the construction of the walls, cut-stones used in the facings (approximately  $0.80\text{ m} \times 0.20\text{ m} \times 0.33\text{ m}$ ) are put together integrating to the rubble core. On the outer facing, the cut-stones are located two abreast and one perpendicular to the facings. Hence, a repetitive decorative texture is provided on the exterior facades of the building. In the 13<sup>th</sup> and 21<sup>st</sup> rows after the lintels of the masonry system, the use of leveling course is observed placing slightly shorter cut-stones (approximately 0.18 m in height) to keep the inner and outer faces of the wall together. The cross walls which separate the chambers of the building provide a bracing for the lateral loads such as wind and earthquake (Mark 1995).

The infill material used in the inner core between the two facings of the walls is composed of soil and stone pieces.

At present, the traces of tooling are observed on the exterior surfaces of cut-stones. There is no trace of any plaster used in or outside surfaces of the walls.

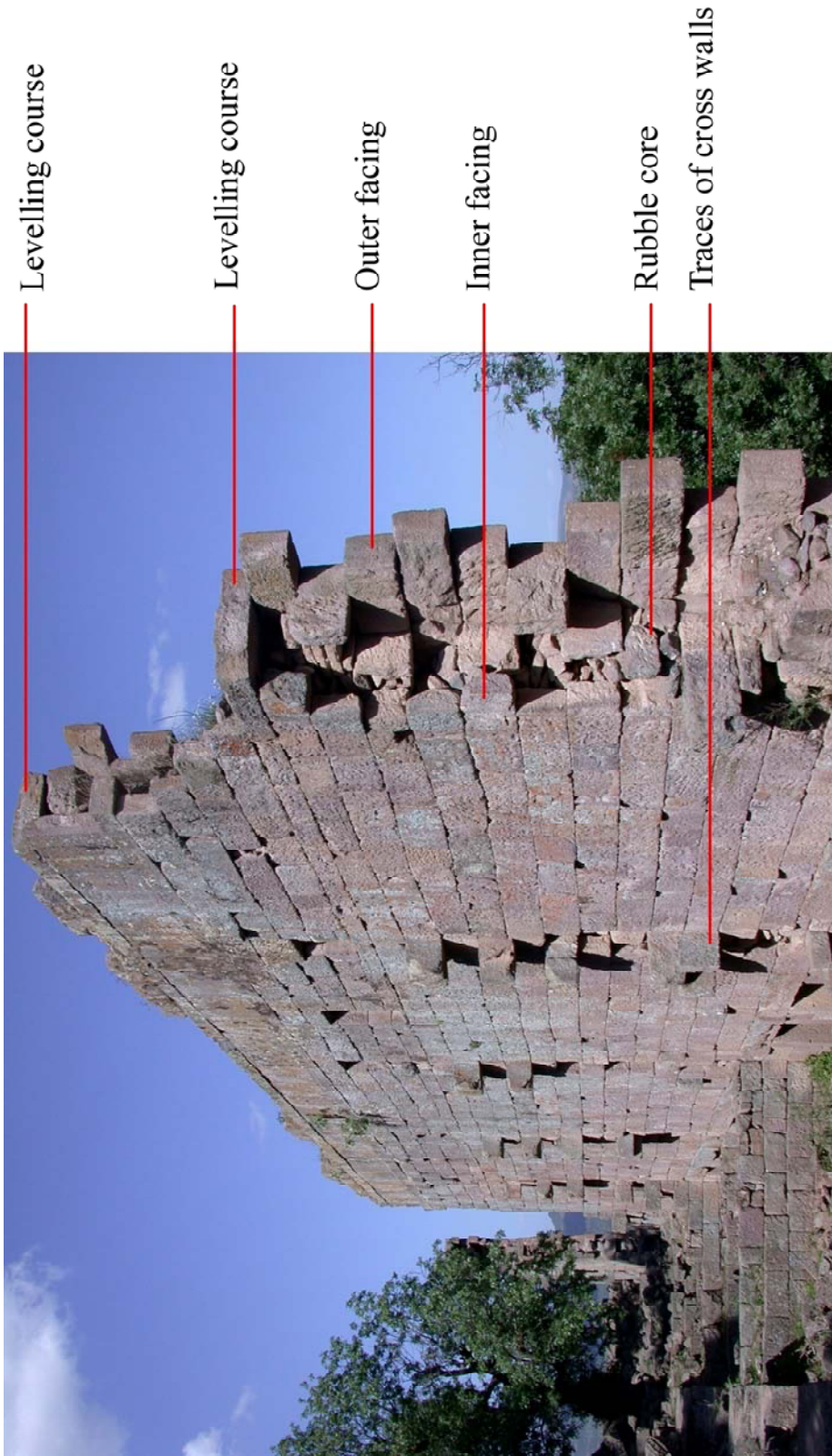


Figure 12. Section of the southeast wall  
(Source: The archives of Aigai excavations 2004)





Figure 13. Section of the Southeast wall showing infill material with soil and pebble stone

### **1.2.1. Stones Used in the Construction of Aigai Agora**

Andesite used in the construction of agora is an igneous rock taken its name from the Andes, the volcanic mountain chain in South America (Press and Siever 2002).

The igneous rocks, which andesite is included, are formed by the solidification of the molten rock magma. Their physical, chemical or mineralogical compositions differ due to solidification period of the magma (Press and Siever 2002). The solids fuse at very high temperatures under the Earth. When the molten rock magma is formed, it rises toward the surface of the Earth because of its low density where the temperature gets lower. By the decrease of the temperature, the minerals in the magma crystallize. Each of the minerals crystallizes at different temperatures, so that the rocks which are formed at different temperatures differ in their physical, chemical and mineralogical characteristics. Firstly, plagioclase feldspar which has high Ca content is crystallized. A chemical reaction occurs between the crystallized matter and magma, and then plagioclase, which has high Na content, is crystallized. Ca and Na content gets lower and the magma forms potassium, aluminum, and orthoclase ( $\text{KAlSi}_3\text{O}_8$ ) by having higher silica content. The rest forms quartz minerals ( $\text{SiO}_2$ ) (Monroe and Wicander 2007). As a result of solidification of magma, different types of igneous rocks are

formed. There are two main ways to determine an igneous rock considering the classification between them (Howe 2001): They are fabric and chemical compositions of the stones. Classification considering the fabric of the rocks is a practical and simple way suitable to be used in the field. The igneous rocks are formed in the different layers, *intrusive igneous rocks* under the Earth's surface; and *extrusive igneous rocks* on the Earth's surface. The slowly solidified intrusive ones are coarsely crystalline rocks because the crystals form over a long period of time. The quickly solidified extrusive rocks exposed to rapid cooling are finely crystalline (aphanitic) rocks. In this classification, andesite is an extrusive volcanic rock which is formed by the rapid cooling of lava on the Earth's surface (Schaffer 1932). The igneous rocks contain 8 main elements in general such as silicon, oxygen, aluminum, iron, magnesium, calcium, sodium and potassium, being 35-75 % silicon and oxygen (Garrels 1951). The classification of these rocks considering the chemical composition is based upon the total silica contents of the igneous rocks: *acid (mafic)* with 66 % silica or more, *intermediate* with 52-66 % silica, and *basic (felsic)* with 52 % or less silica content (Howe 2001). In this classification, andesite is an intermediate igneous rock.

Considering all the classifications mentioned above, andesite is an intermediate igneous rock with 52-65 % silica content. The dominant mineral is plagioclase feldspar with little or no quartz. It also may contain the mafic minerals such as biotite, amphibole and pyroxene. It is a fine grained (aphanitic) extrusive rock which is formed by the solidification of volcanic lava by rapid cooling (Press and Siever 2002). When the physical characteristics of andesite are considered, its specific gravity is about 2.2 to 2.7, and porosity values vary from 3 percent to 6 percent (Howe 2001).

The studied rock type andesite was studied by Saito considering the weathering of igneous rocks in 1981. Then, it was studied by John Allen Howe in the concept of rock classification including their characteristics and weathering problems in 2001. Press and Siever mentioned andesite in their study about formation of rock types, classification and their weathering in 2002. Lee and Yi studied the weathering problems of building stones of a case study including andesite in a case study in 2006. In 1997, Karpuz and Paşamehmetoğlu studied weathering problems of Ankara andesite. Andesite is also studied by Arıkan, Ulusay and Aydın in 2007. In 1995, Koca studied the characteristics of abandoned andesite quarries in and around İzmir city center. Yavuz studied the deterioration problems of andesite used as a pavement stone in the city centre of İzmir in 2006.

### 1.2.2. Weathering of Andesite

Weathering is defined as the physical disintegration and chemical decomposition of the stone (Schaffer 1932). The key factors that influence the weathering of materials are the nature of the stone and the environment where they are located (Charola 2004). The chemical and mineralogical compositions and physical properties such as density and porosity are the main factors that determine the nature of the stone. As a result of weathering, the material characteristics of the stone are altered. A reduction in strength and structural instability and an increase in deformability is observed in the stone while changing its permeability, and affecting the weathering indices of the stone (Arıkan, et al. 2007). It may also cause discoloration on materials (Lee and Yi 2006).

Weathering is observed in two forms on stone: chemical weathering and physical weathering.

*Chemical weathering* is the process by which the minerals of the stone are altered or dissolved as a result of chemical reactions between the minerals and air or water.

Kaolinisation is an important chemical weathering which is observed on igneous rocks with Na, Ca and K-feldspar content (Schiavon 2006). Feldspar, which is a common mineral in many igneous rocks such as andesite, is altered as a result of hydration. The mineral gains water during the chemical reactions and kaolinite clay (a hydrous aluminum silicate) forms (Reaction a). In this sense, water is an important factor in the weathering of feldspars (Press and Siever 2002).

a) Orthoclase ( $\text{KAlSi}_3\text{O}_8$ ) + Water  $\rightarrow$  Kaolinite clay + Potassium ions + Silica ( $\text{SiO}_2$ )

The role of carbon dioxide is another important factor in the weathering of feldspars. Carbon dioxide gas ( $\text{CO}_2$ ), which exists in the atmosphere, is dissolved in the rainwater and carbonic acid ( $\text{H}_2\text{CO}_3$ ) is derived (Reaction b). As a result of the chemical reaction between feldspars and carbonic acid, dissolved kaolinite, dissolved silica, dissolved potassium and dissolved bicarbonate ions occur (Press and Siever 2002).

b)  $2 \text{KAlSi}_3\text{O}_8 + 2 \text{H}_2\text{CO}_3 + \text{H}_2\text{O} \rightarrow \text{Al}_2\text{Si}_2\text{O}_5(\text{OH})_4 + 4\text{SiO}_2 + 2\text{K}^+ + 2\text{HCO}_3^-$

If the stone is buried, there are some other factors that influence the weathering of feldspar. In soil, an acidic environment occurs because of the presence of bacteria, lichens, mosses and biological growth. As a result, stones are exposed to not only water but also acid under the soil (Press and Siever 2002).

The minerals absorb water during the hydration and lose silica as a result of weathering. Sodium, potassium, calcium and magnesium ions and clays form. However, some silicates such as quartz, which is one of the slowest weathering minerals, do not leave any clay residue. Andesite is an igneous rock containing various minerals. Hence the chemical reactions of these minerals with water and air cause chemical deterioration on this stone.

There are also other chemical weathering types observed on stones such as the alteration of iron silicates to iron oxides by dissolution of CO<sub>2</sub> and its reaction with iron silicates and oxygen in the air (Press and Siever 2002). Also, the effect of air pollution should be regarded as an important factor on the chemical weathering of stones (Schaffer 1932). If the stone is a calcareous stone, it may cause the formation of gypsum because of SO<sub>2</sub> reaction with acid gases in the air. These acid gases may also cause the chemical reactions with andesite. As a result of these reactions, soluble salts such as sulphates, chlorides, nitrates, nitrites and phosphates may form on andesite which may accelerate the weathering process (Tokmak 2005).

*Physical weathering* is the process which the rock becomes fragmented by various physical processes. As a result of physical weathering, cracks and breakage, fragmental losses, surface exfoliation, peel-off, wear and tear may form (Lee and Yi 2006). The soil grains are derived with the physical weathering of cracked particles. These soil grains may be moved from the stone's surface by erosion or they may increase the weathering rate in the crack where they are situated (Press and Siever 2002).

The breakage may form in the rocks because of various reasons as listed below (Press and Siever 2002):

- Natural zones of weakness in the heterogeneous stones,
- Activities made by the organisms as producing acid and causing chemical weathering,
- Forming roots causing physical weathering by the force of the growing root system,

- Crystallization of minerals such as calcium carbonate or salt,
- Clay formation,
- Climatic conditions and alternating heat and cold and frost wedging,
- Physical weathering and erosion,
- Damages made by humans or natural disasters.

### **1.3. Climatic Characteristics of the Site**

The climatic condition (temperature, relative humidity, wind and rain that the building is exposed to) of the site where the monument is located is one of the key factors that affect the weathering of stone (Charola 2004). In this point of view, the weathering problems of the building stones in Aigai Agora were discussed considering the climatic conditions of the site. The climatic condition of the site was evaluated considering the data taken from The General Directorate of State Meteorological Affairs, Ankara recorded at the closest meteorological station located in Manisa District of Manisa city which is 71.0 m high from sea level. The graphs of the recorded meteorological data between 1996 and 2006 containing monthly average values of temperature, dew point temperature, relative humidity (Figure 14), rainfall (Figure 15) and wind speed (Figure 16), and temperature and relative humidity values at 7.00, 14.00 and 21.00 (Figure 17) in the same time period in Manisa district of Manisa city, where Aigai is located, were drawn and evaluated.

During the winter months as December, January and February, the ambient temperatures are minimum which change between 5-15°C considering the whole year and dew point temperatures are below 5°C, not lower than 0°C. The relative humidity values change between % 70 and % 80 and the rainfall shows the optimum values higher than 100 mm per meter square. The wind speed changes between 1.4-1.8 m/sec. In June, July and August, that are the summer months, the ambient temperatures show the optimum values of the whole year which change between 25-35°C and dew point temperatures show the optimum values, either, changing between 10-15°C. Relative humidity values change between % 40 and % 60 and monthly average values of rainfall

is minimum during these months lower than 20mm per meter square. The wind speed changes between 1.8-2.0 m/sec.

The monthly average values of ambient temperature and relative humidity recorded at 7:00, 14:00 and 21:00 were also evaluated in order to define approximately when the optimum weathering occurs in a day in different seasons. Considering the results, ambient temperatures are lowest at 7:00 and highest at 14:00; and relative humidity is lowest at 14:00 and highest at 7:00 both in winter and in summer.

The number of frosty days were also investigated (Figure 18). The total rate of frosty days are approximately 21 days in a year considering the average monthly frosty days between the years 1996 and 2006. The results show that winter months, especially January, are the months which frosty days are mostly seen in the area.

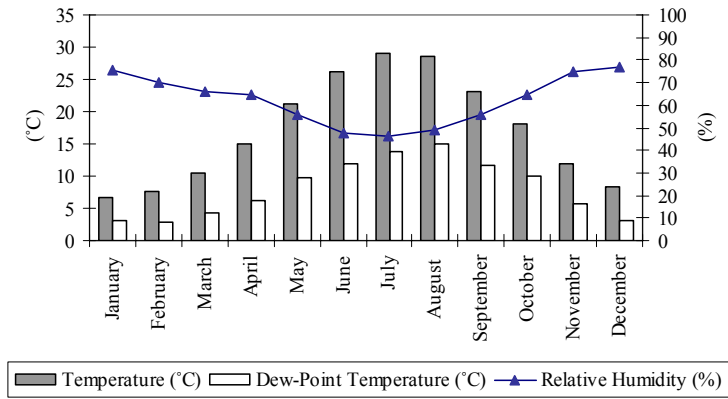


Figure 14. Average values of the average monthly values of ambient temperature, relative humidity and dew-point temperature between the years 1996 and 2006 (Source: General Directorate of State Meteorological Affairs Ankara)

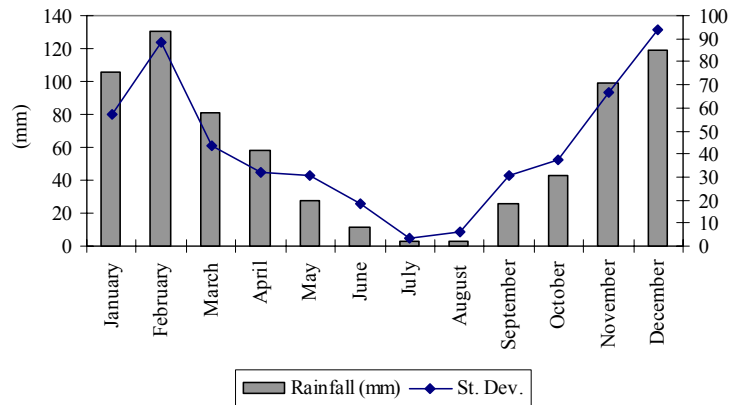


Figure 15. Average values of average monthly values of rainfall between the years 1996 and 2006 (Source: General Directorate of State Meteorological Affairs Ankara)

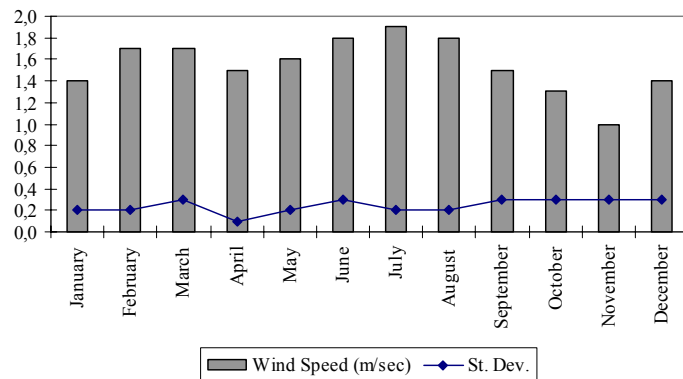
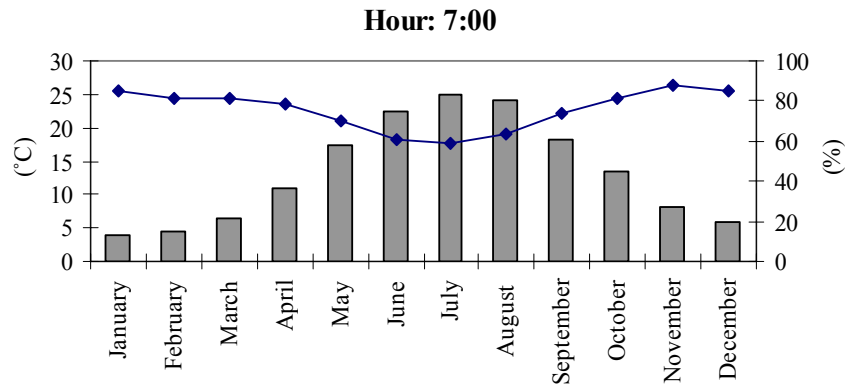
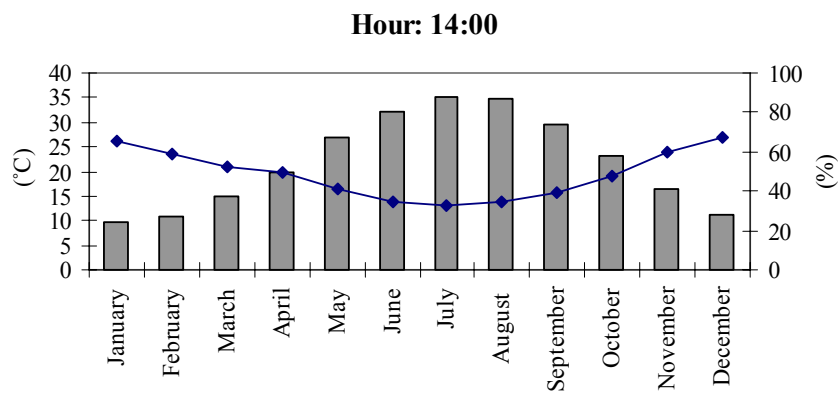


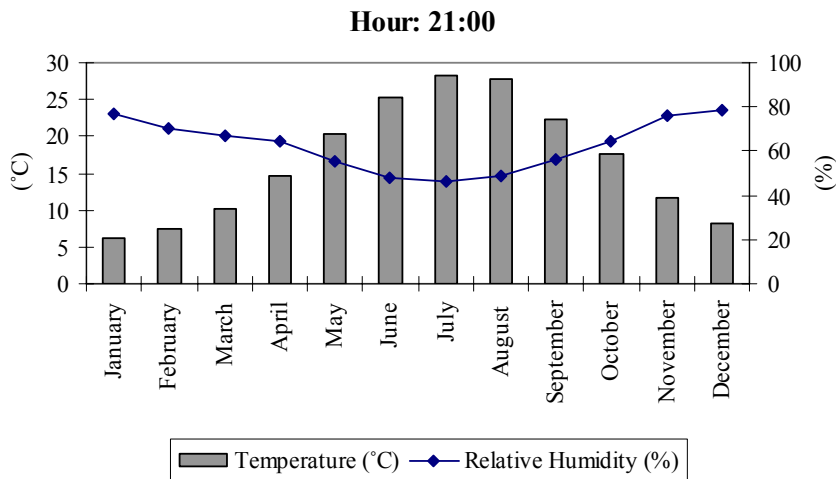
Figure 16. Average values of the average monthly values of windspeed between the years 1996 and 2006 (Source: General Directorate of State Meteorological Affairs Ankara)



a)



b)



c)

Figure 17. Average values of the average monthly values of ambient temperature and relative humidity between the years 1996 and 2006; hour: 7:00 a), 14:00 b), 21:00 c) (Source: General Directorate of State Meteorological Affairs Ankara)



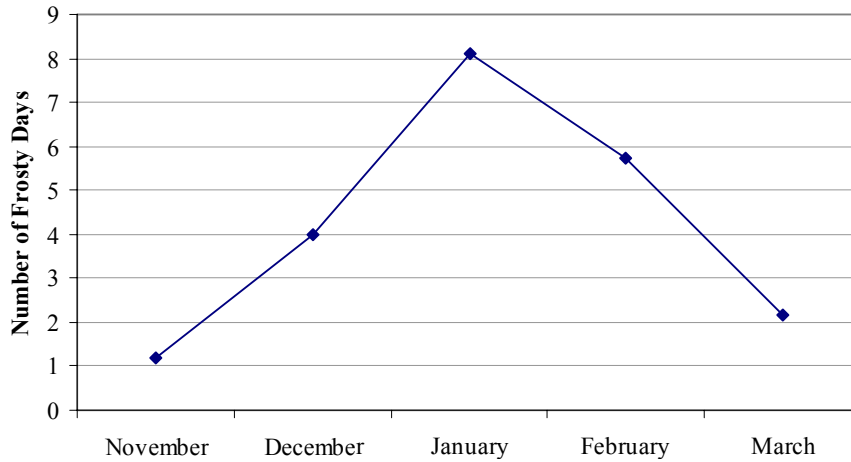


Figure 18. Average values of the average monthly frosty days between the years 1996 and 2006 (Source: General Directorate of State Meteorological Affairs Ankara)

Condensation occurs when the ambient temperature is close to the dew point temperature. When the average seasonal values are considered, the possibility of condensation of water on the building stones is higher during the winter months, when rainfall is maximum and wind speed is minimum, which increase the humidity in the air (İpekoğlu, et al. 2005). As well, relative humidity is higher than % 70 in winter which increases the deterioration problems of building stones in the area. When the ambient temperature and relative humidity are evaluated considering different time intervals in a day, the condensation possibly occurs mostly at 7:00 because of the high relative humidity values and low temperatures.

#### 1.4. Aim of the Study

Since there are several fields to be studied in an archaeological site, the conservation work should be carried out in a multidisciplinary way to meet all the requirements of an archaeological study. In this respect, the documentation and evaluations in each province should be made in detail to begin an excavation in an archaeological site. By this way, architectural, aesthetic, cultural, structural and material characteristics of the monuments could be deciphered precisely and a basis could be

formed for the conservation interventions which will be applied on an archaeological monument.

In this sense, determination of material characteristics and weathering problems of the building materials is an important phase of conservation work.

The aim of this study is to determine the weathering forms observed on andesite used as building stone in the construction of the agora with their reasons. The material characteristics of andesite and infill material used in the construction of the building are determined in the scope of the study. These are the preliminary studies for the conservation works of agora. In the future works, other essential studies should be made precisely for the conservation of Aigai Agora.

## **CHAPTER 2**

### **SITE SURVEY**

In the site survey of the study held in August 2007, sketches of southeast facade of the Agora Building were prepared, and the measurements of the details of doors and windows, and structural elements were done using traditional methods.

#### **2.1. Visual Analysis of Stone Weathering Observed on the Southeast Wall of Aigai Agora**

The detailed material deteriorations were documented visually using mapping method on the sketches. Photographical documentation was made during the site survey.

The sketches of the building were taken from the excavation archives and the drawing of southeast elevation, which should be regarded as a scaled sketch of the building, was revised by the author. The mapping of the southeast facade was made on the revised southeast elevation. The photographs taken in the site were scaled in ArchiCAD 9.0 program using the dimensions of the building, and the deteriorated parts of the stones on the southeast facade were shown using the dimensions and scaled photographs in AutoCAD 2007 program.

Considering the results of the site survey and office works, the material deteriorations were classified considering the studies of Fitzner (Fitzner and Heinrichs 2001). The weathering forms observed on the wall were determined as shown Table 1.

Table 1. The observed weathering forms of stone on the Southeast wall of Agora

<b>Loss of stone material</b>	<b>Relief</b> Morphological change of the stone surface due to partial or selective weathering (Figure 19, Figure 20).
	<b>Back weathering</b> Uniform loss of stone material parallel to the original stone surface (Figure 21, Figure 22).
	<b>Break out</b> Loss of compact stone fragments (Figure 23, Figure 24).
<b>Discoloration and deposit</b>	<b>Coloration</b> Chromatic alteration / coloring due to chemical weathering of minerals (e.g. oxidation of iron and manganese compounds), due to intrusion / accumulation of coloring matter or due to staining by biogenic pigments (Figure 25).
	<b>Microbiological colonization</b> Colonization by microflora (fungi, algae, lichen) and bacteria. Biofilms (Figure 26, Figure 27).
	<b>Black Crust</b> Compact deposit, grey- to black-colored, changing the morphology of the stone surface (Figure 28).
	<b>White Deposition</b> Compact deposit, white colored (Figure 25, Figure 29).
	<b>Higher Plants</b> Plant and tree growth (Figure 30, Figure 31).
<b>Detachment</b>	<b>Granular disintegration</b> Detachment of individual grains or small grain aggregates (Figure 32, Figure 33).
	<b>Scaling</b> Detachment of larger, platy stone pieces parallel to the stone surface, but not following any stone structure (Figure 34, Figure 35).
	<b>Detachment of black crust</b> Detachment of a colored crust tracing the stone surface (Figure 36, Figure 37).
	<b>Fissures</b> Individual fissures or systems of fissures due to natural or constructional causes (Figure 38).



Figure 19. Relief observed on the stone surfaces of Agora

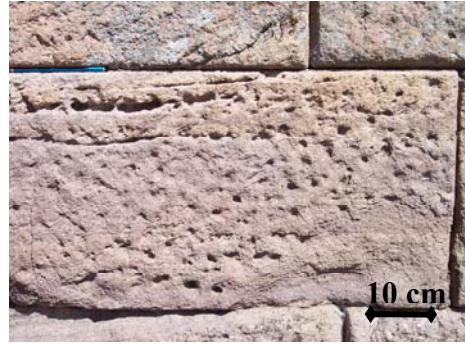


Figure 20. Relief observed on the stone surfaces of Agora



Figure 21. Back weathering observed on the stone surfaces of Agora



Figure 22. Back weathering observed on the stone surfaces of Agora



Figure 23. Break out observed on some parts of the building stones of Agora



Figure 24. Break out observed on some parts of the building stones of Agora

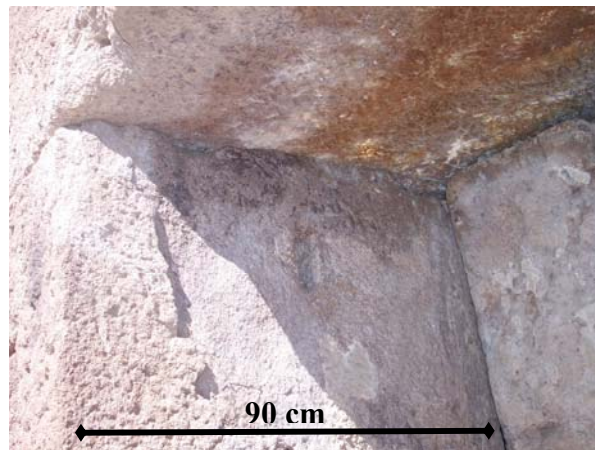


Figure 25. Coloration and white deposition observed on the stone surfaces of Agora



Figure 26. Microbiological colonization observed on the stone surfaces of Agora



Figure 27. Microbiological colonization observed on the stone surfaces of Agora



Figure 28. Black crust observed on the stone surfaces of Agora



Figure 29. White deposition observed on the lintels of door and window openings of Agora



Figure 30. Higher plants observed on some parts of Southeast facade of Agora



Figure 31. Higher plants observed on some parts of Southeast facade of Agora



Figure 32. Granular disintegration observed on the stones of Agora



Figure 33. Granular disintegration observed on the stones of Agora



Figure 34. Scaling observed on the stone surfaces of Agora



Figure 35. Scaling observed on the stone surfaces of Agora



Figure 36. Detachment of black crust observed on the stone surfaces of Agora

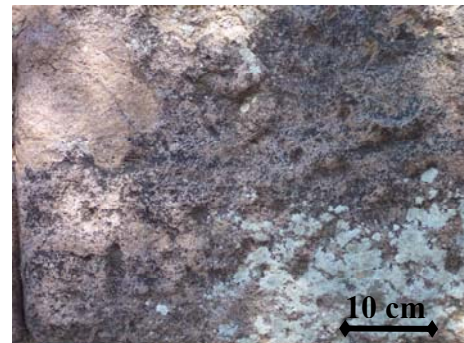


Figure 37. Detachment of black crust observed on the stone surfaces of Agora





a



b

Figure 38. Cracks a) and fissures b) observed on the stones of Agora

## 2.2. Mapping of Weathering Forms Observed on the Southeast Wall of Aigai Agora

Considering the visual observations on site and results of experimental study, the weathering forms are observed in different forms on the building stones in the southeast wall of Aigai Agora (Figure 39) The weathering forms observed on stone surface are detachment, discoloration and deposit, and loss of stone material. These weathering forms are classified in different headings as follows considering Fitzner's classification on the weathering of stone (Fitzner and Heinrichs 2001):

- *Detachment* in the forms of fissures, scaling, and detachment of black crust;
- *Discoloration and deposit* in the forms of coloration, microbiological colonization, black crust, white deposition and higher plants;
- *Loss of stone material* in the forms of relief, granular disintegration, back weathering and break out on the surface of the stones.

In agora, each of the weathering forms occurs because of various reasons:

The detachment in stone may form because of various reasons such as heterogeneous nature of stone, climatic factors as freeze-thaw cycles, swelling of clays by the effects of dampness or the problems in the distribution of load on the structure. Chemical reaction occurred in stone or microbiological growth on the inner crack surfaces may be the causes of detachment of stone particles.

Discoloration and deposit formation may have various physical and chemical reasons. Coloration is mostly due to microbiological growth, and microbiological growth is formed as a result of dampness and clay presence on stone. Black crust, which is observed on the stone surfaces maximum 1.00 m high from the ground, is thought to be made by human fires. The black crust formation causes detachment on stone surface and it causes loss of material on the stone surface, too. White deposition is due to salt crystallization on a limited area on the wall. White deposition observed from gypsum crystallization is indicated on the side and top surfaces of door and window openings.

Loss of stone material occurred due to various reasons. Relief is the most common weathering form observed in this building. It is formed on the whole surface of the wall. At the corner stones of the wall at the southeast and southwest corners of the building mass, relief is not observed. Also, there is not a tooling application on these

corners of the stones (Figure 40). Besides the various factors that cause relief on stone surface such as physical and chemical factors, biodegradation or clays moved with wind from surrounding area or derived in the origin of the stone, the formation of relief was accelerated because of tooling applied on the cut-stone surfaces. In order to provide a texture on the stone surface by tooling, the stone is damaged. As a result, the stone surface that rainfall or other atmospheric conditions affect directly is enlarged and the weathering process is accelerated (Spock 1953). Another form of loss of stone material which is granular disintegration is due to the heterogeneous nature of stone. Andesite is a volcanic rock derived from the crystallization of magma. During the cooling process, different zones and soft beds are able to be formed in the same region (Schaffer 1932). In this sample, the same formation is observed on the surface of the wall. While the stone surfaces are in sound conditions, on some parts of the facade, there are weathered andesite samples which occur in the form of granular disintegration because of the presence of a soft bed and efflorescence in the building stones of Agora (Figure 41).

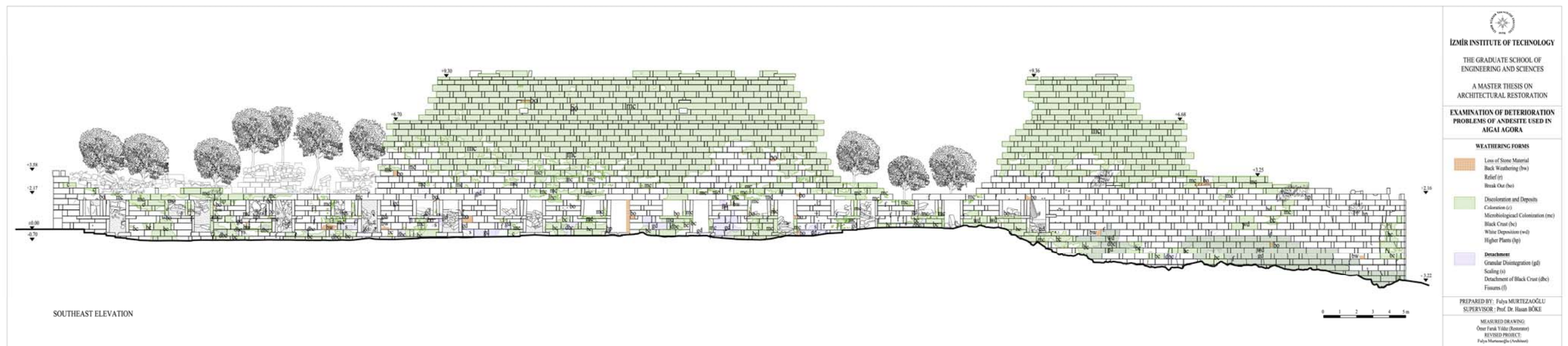


Figure 39. Mapping of weathering forms observed on the Southeast Facade of the building



Figure 40. Relief and traces of tooling on stone surfaces and the sound corner parts without tooling at the southeast corner of the building



Figure 41. Effect of efflorescence and granular disintegration

### 2.3. Structural Problems Observed on the Southeast Wall of Aigai Agora

The determination of the structural problems on agora wall is based on visual observations. The roof and first and second floors of the building were collapsed because of lack of maintenance and damage by man. The collapsed building stones of the upper floors lie in the chambers of the ground floor and cause pressure on the southeast wall of the building which is clearly observed from the east corner of the building. Bending of upper parts of the wall to the southeast direction and cracks formed in this corner are important structural problems that should be solved

immediately (Figure 42). The southeast wall is collapsed especially on the first and second floor levels. Some of cut-stones on the upper parts tend to fall down. On the ground floor, there are fissures formed on the lintels of some door and window openings whose reasons are thought to be the problems occurred in the distribution of loads after the collapses (Figure 43).

In order to form an appropriate treatment approach for the conservation of the building, the determination of structural problems of the southeast wall and the building must be determined by the necessary structural analysis.

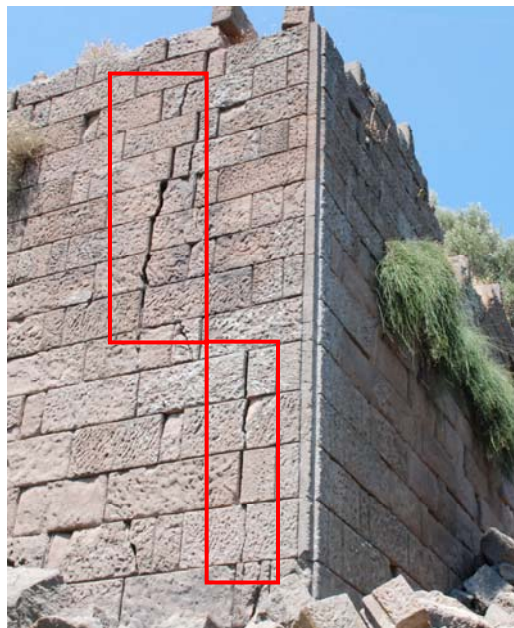


Figure 42. Cracks formed on the eastern corner of the building



Figure 43. Fissures formed on the lintels of door and window openings

## CHAPTER 3

### EXPERIMENTAL STUDY

In this work, the laboratory studies aimed to characterize the chemical, mineralogical and physical properties of the andesite used in the construction of Agora with their deterioration problems and their reasons.

#### 3.1. Sampling

The andesite samples were collected from the sound and deteriorated parts of the walls, and the soil sample used in the rubble core was collected without damaging the building in the site survey in 2007 (Figure 44, Figure 45, Figure 46, Figure 47, Figure 48). The collected samples were put in pockets separately and named considering an order in nomenclature (Table 2). According to the nomenclature of the samples, the first letter represents agora (A), the second represents the material type if it is the building stone or infill material (St: Andesite, S: Soil from the infill material), the third represents the material number (as 1, 2, 3), and the last represents the location of the sample on the material (E: Exterior Surface, Cr: Inner Crack Surface, I: Interiors). There may be a following code after the fourth one which represents the kind of the material derived on the stone samples (F: Soil fraction less than 53  $\mu\text{m}$  which was derived on the stone surface).

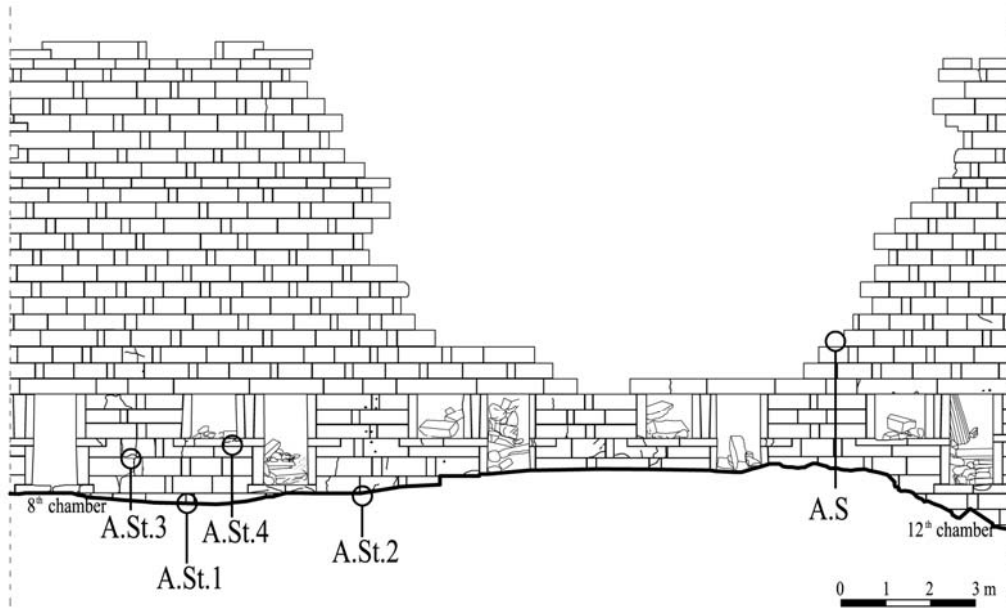


Figure 44. Partial elevation of Agora, showing where the samples were collected



Figure 45. Collapsed building stones, showing where the andesite samples were collected (A.St.1 and A.St.2)



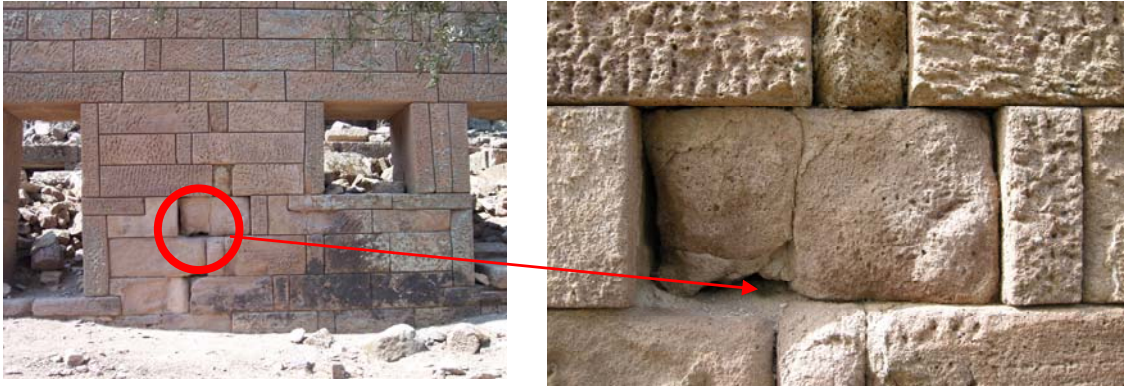


Figure 46. Southeast facade of the wall, showing where the andesite samples were collected (A.St.3)



Figure 47. Southeast facade of the wall, showing where the andesite samples were collected (A.St.4)







Figure 48. Rubble core, showing where infill materials were collected (A.S)



Figure 49. Lintel of 7<sup>th</sup> chamber showing where samples of efflorescence were collected (A.Eff.1)

Table 2. Samples collected from the site

Sample	Sample Definition
<p><b>A.St.1</b></p> 	<p>Andesite from the ground beneath the fallen building stones lying in front of the building in order to define the material characteristics of sound andesite in the site</p>
<p><b>A.St.1.I</b></p>	<p>Inner part of the stone in a sound condition</p>
<p><b>A.St.2</b></p> 	<p>Andesite from the ground beneath the fallen building stones lying in front of the building</p>
<p><b>A.St.3</b></p>  <p>(E) Exterior Surface      (Cr) Inner Crack Surface</p>	<p>Weathered andesite from the surface of the stones between the 8<sup>th</sup> and 9<sup>th</sup> chambers</p>
<p><b>A.St.3.Cr.F</b></p>	<p>Soil fraction less than 53 <math>\mu\text{m}</math> which is separated from the inner crack surface of the weathered stone</p>
<p><b>A.St.3.E.</b></p>	<p>Exterior surface of the scaled stone piece</p>
<p><b>A.St.3.I.</b></p>	<p>Inner part of the scaled stone piece</p>
<p><b>A.St.3.Cr.</b></p>	<p>Inner crack surface of the scaled stone piece</p>
<p><b>A.St.4</b></p>  <p>(E) Exterior Surface      (Cr) Inner Crack Surface</p>	<p>Weathered andesite from the surface of the wall of the 9<sup>th</sup> chamber</p>
<p><b>A.Eff.1</b></p>	<p>Efflorescence from the surface of lintel of 7<sup>th</sup> chamber</p>
<p><b>A.S.</b></p>	<p>Infill material from the inner core of the wall</p>
<p><b>A.S.F</b></p>	<p>Soil fraction less than 53 <math>\mu\text{m}</math> separated from the infill material</p>
<p><i>A: Agora; S: Soil fraction taken from infill material, St: Stone Sample, andesite, Eff: Efflorescence; E: Exterior surface, I: Sound inner part; Cr: Inner crack surface, F: Soil fraction less than 53 <math>\mu\text{m}</math></i></p>	

## 3.2. Experimental Methods

Various laboratory tests were applied on stone and infill material samples during the experimental studies. The material characteristics and deterioration problems of the building materials were investigated.

The determination of basic physical properties of sound andesite and particle size distribution of infill material were determined. Mineralogical and chemical compositions and microstructural properties with deterioration problems and their reasons, weight loss by thermogravimetric analysis, and salt content in the materials were analyzed for sound and weathered andesite samples and infill material.

### 3.2.1. Determination of Basic Physical Properties of Andesite

The values of bulk density ( $\text{g/cm}^3$ ), which is the ratio of the mass to its bulk volume, and porosity (%), which is the ratio of the pore volume to the bulk volume, (RILEM 1980) of andesite samples were determined by RILEM standard test methods. Four unweathered and four weathered samples were first dried in an oven at  $40^\circ\text{C}$  for 24 hours, and their dry weights ( $M_{\text{dry}}$ ) were determined by a precision balance (AND HF-3000G). Then, the saturated weights ( $M_{\text{sat}}$ ) and archimedes weights ( $M_{\text{arch}}$ ) of the samples were determined by saturating them with distilled water in a vacuum oven (Lab-Line 3608-6CE Vacuum Oven) and weighing by a precision balance using hydrostatic weighing method in distilled water. The bulk densities (D) and porosities (P) of the samples were determined using the formulas below:

$$D (\text{g/cm}^3) = M_{\text{dry}} / (M_{\text{sat}} - M_{\text{arch}})$$

$$P (\%) = [(M_{\text{sat}} - M_{\text{dry}}) / (M_{\text{sat}} - M_{\text{arch}})] \times 100$$

where;

$M_{\text{dry}}$  : Dry Weight (g)

$M_{\text{sat}}$  : Saturated Weight (g)

$M_{\text{arch}}$  : Archimedes Weight (g)

$M_{\text{sat}} - M_{\text{dry}}$  : Pore Volume

$M_{\text{sat}} - M_{\text{arch}}$  : Bulk Volume

The weathered andesite samples were prepared as transverse thin sections from exterior surface to the inner parts. The crack and void areas were calculated in detail using the BSE images of these samples. Crack formation on andesite surfaces were determined considering the porosity change (Tuğrul 1995).

### **3.2.2. Determination of Particle Size Distribution of Infill Material**

Particle size distributions of aggregates in the infill material of masonry walls were determined by sieve analysis (Teutonico 1988). The sample was sieved through a series of sieves having the sieve sizes of 125  $\mu\text{m}$ , 250  $\mu\text{m}$ , 500  $\mu\text{m}$ , 1180  $\mu\text{m}$  by using an analytical sieve shaker (Retsch AS200). Each of the aggregates retained on the sieves were weighed separately and their percentages in the soil were calculated. The images of the aggregates were taken using a zoom stereo microscope (Olympus SZ40) with a video camera, a photo micrographic system and a computer and their physical properties were examined visually.

### **3.2.3. Determination of Mineralogical and Chemical Compositions of Andesite and Infill Material**

Stone and soil which was used as infill material were ground to particles less than 53 $\mu\text{m}$ . X-ray Diffraction (XRD) analysis were applied on these samples using a Philips X-Pert Pro X-ray Diffractometer in order to define mineralogical compositions of the building materials including the sound and weathered parts.

The stone samples taken from the unweathered and weathered parts of the stone were ground to particles less than 53 $\mu\text{m}$  to determine their chemical compositions using the Philips XL 30S-FEG Scanning Electron Microscope (SEM) equipped with X-Ray Energy Dispersive System (EDS). The soil particles which were derived on the inner

crack surface of stone and soil particles of infill less than 53 $\mu$ m were ground and pressed into pellets and analyzed using the same method.

The soil samples less than 53 $\mu$ m were ground, mixed with 100 unit of KBr to 1 unit of sample, and pressed into pellets. KBr and sample pellets were heated to 100°C to remove the absorbed water. Samples were analyzed using Perkin Elmer FT-IR System Spectrum BX by scanning each of the samples four times in order to evaluate their chemical properties.

#### **3.2.4. Determination of Microstructural and Petrographical Characteristics of Andesite**

The microstructural properties of unweathered andesite were determined by thin section analyses. The sound andesite samples were impregnated by epoxide resin in Lab-Line 3608-6CE Vacuum Oven for 24 hours. The samples were cut to 2 mm or 3 mm thick slices using BUEHLER Low Speed Saw. The thicknesses of the sections were reduced to nearly 30  $\mu$ m. The prepared samples were analyzed using Nikon ECLIPSE E400 POL Polarized Microscope and Philips XL 30S-FEG Scanning Electron Microscope (SEM).

#### **3.2.5. Determination of Weight Loss of Andesite by Thermogravimetric Analysis**

The weight loss in stone and soil were determined by thermogravimetric analysis (TGA) using Perkin Elmer Diomand TG/DTA in static nitrogen atmosphere at a temperature range of 25-1000 °C with a heating rate of 10°C/min. Soil and stone samples were ground to particles less than 53 $\mu$ m. While the stone samples were ground to particles less than 53 $\mu$ m to use in TGA analysis, a different method was applied on soil sample in order to separate particles less than 53 $\mu$ m. After 30g of soil sample was

decomposed in distilled water, finer particles were filtered to use in the laboratory experiments and TGA analysis.

### 3.2.6. Determination of Salt Content

The salt content and percentage in the materials were determined in order to evaluate the weathering problems of andesite.

The first step was to determine the percentage of soluble salts by using an electrical conductivity meter (WTW MultiLine P3 pH/LF) (Black 1965). 1.0 g of samples were dissolved in 50ml distilled water and filtered. After the conductivities of the solutions were measured, the percentages of soluble salts were calculated using the formula below:

$$\text{Soluble Salts (\%)} = [(A \times V_{\text{sol}}) / 1000] \times [100 / M_{\text{sam}}]$$

where;

A : Salt concentration (mg/l) = 640 x EC

EC : Electrical conductivity measured by electrical conductivity meter  
(mS/cm = mmho/cm)

640 : Constant

Vsol : Volume of the solution (ml)

Msam : Weight of the sample (mg)

The principle anions of soluble salts were also determined qualitatively by applying spot tests on the same solutions in order to determine which anions of sulphate ( $\text{SO}_4^{-2}$ ), chloride ( $\text{Cl}^-$ ), nitrate ( $\text{NO}_3^-$ ), carbonate ( $\text{CO}_3^{-2}$ ) and phosphate ( $\text{PO}_4^{-3}$ ) may be present in the samples (Black 1965, Arnold 1983 and Teutonico 1988).

## **CHAPTER 4**

### **RESULTS AND DISCUSSION**

In this chapter, basic physical properties, microstructural features, mineralogical and chemical compositions of sound and weathered andesite and infill material used in the construction of agora were expressed and discussed.

#### **4.1. Characteristics of Andesite used in the Construction of Aigai Agora**

##### **4.1.1. Basic Physical Properties of Andesite**

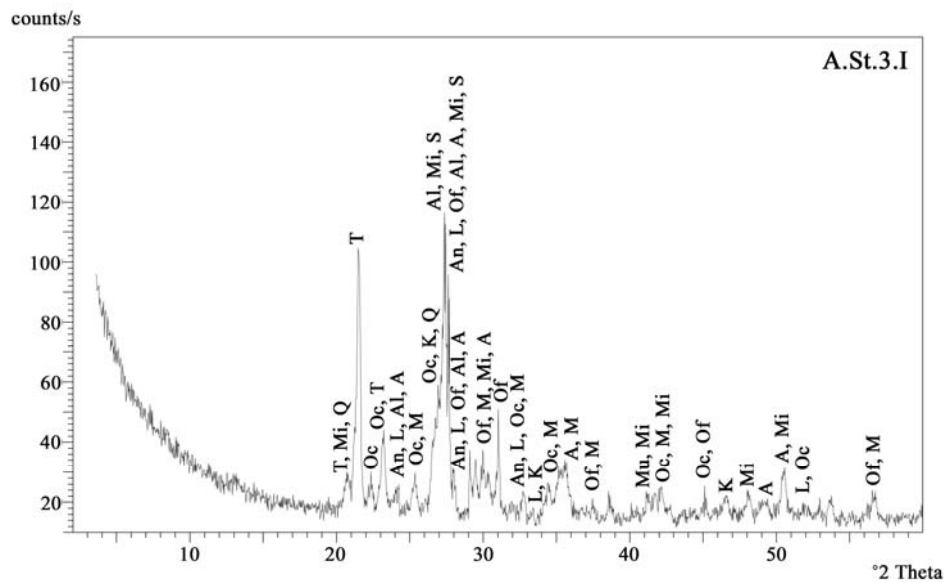
The density and porosity values of unweathered and weathered andesite were determined by RILEM standard test methods. The density of sound andesite samples varied between 2.3 g/cm<sup>3</sup> and 2.4 g/cm<sup>3</sup>. Porosity values of the same samples were in the range of 7.7-8.2 %. These values are comparable with the values assigned in the previous studies on andesite (Howe 2001).

##### **4.1.2. Mineralogical Composition of Andesite**

Mineralogical composition of andesite has been determined by XRD analysis. XRD results show that sound andesite used in the building was composed of



tectosilicate minerals, phyllosilicate minerals, inosilicate minerals and isosilicate minerals. Tectosilicate minerals indicated are feldspar groups as plagioclase feldspars (aluminosilicates) albite, andesine, anorthite and labradorite; alkali feldspars sanidine, orthoclase and microcline; and quartz group as quartz and tridymite. Phyllosilicate mineral is a mica group mineral as muscovite. Inosilicate minerals are mullite and orthoferrosilite. Isosilicate mineral is kyanite (Figure 50).



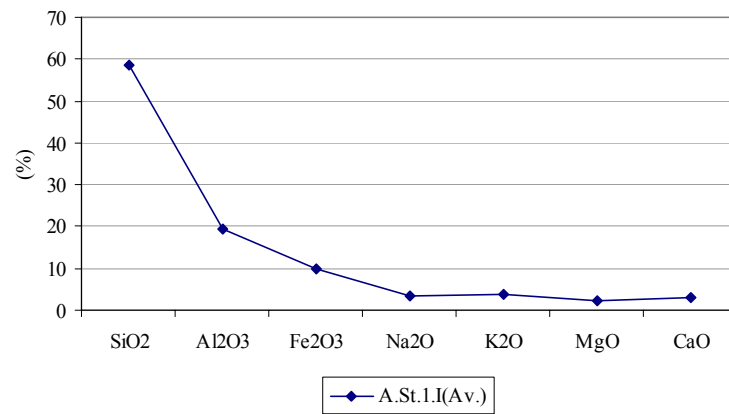
A: Andesine (79-1148), Al: Albite high (83-1608), An: Anorthite (70-0287), K: Kyanite (72-1441), L: Labradorite (83-1368), M: Muscovite (76-0668), Mi: Microcline (76-1238), Mu: Mullite (02-1160), Oc: Orthoclase (75-1190), Of: Orthoferrosilite (83-0668), Q: Quartz (83-2468), S: Sanidine (19-1227), T: Tridymite (42-1401)

Figure 50. XRD pattern of sound andesite sample from the inner part

### 4.1.3. Chemical Composition of Andesite

Chemical composition of andesite has been determined by SEM – EDS analysis. Unweathered andesite samples were composed mainly of silicon dioxide ( $\text{SiO}_2$ ), aluminum oxide ( $\text{Al}_2\text{O}_3$ ) and iron oxide ( $\text{Fe}_2\text{O}_3$ ). The minor elements were sodium

oxide ( $\text{Na}_2\text{O}$ ), potassium oxide ( $\text{K}_2\text{O}$ ), magnesium oxide ( $\text{MgO}$ ), calcium oxide ( $\text{CaO}$ ) and phosphorus pentoxide ( $\text{P}_2\text{O}_5$ ) (Figure 51). Igneous rocks are classified considering their silica content: acid (mafic) with 66 % silica or more, intermediate with 52-66 % silica, and basic (felsic) with 52 % or less silica content (Howe 2001). Andesite used in agora is an intermediate igneous rock with 59 %  $\text{SiO}_2$  content.



a)

Sample	$\text{SiO}_2$	$\text{Al}_2\text{O}_3$	$\text{Fe}_2\text{O}_3$	$\text{Na}_2\text{O}$	$\text{K}_2\text{O}$	$\text{MgO}$	$\text{CaO}$
A.St.1.I <sub>(1)</sub>	59,67	19,57	9,63	3,19	3,41	2,07	2,46
A.St.1.I <sub>(2)</sub>	55,09	18,82	12,78	3,9	3,94	2,67	2,8
A.St.1.I <sub>(3)</sub>	60,65	19,76	6,92	3	4,31	2,06	3,29
A.St.1.I <sub>(Av.)</sub>	58,5 ± 3,0	19,4 ± 0,5	9,8 ± 2,9	3,4 ± 0,5	3,9 ± 0,5	2,3 ± 0,3	2,9 ± 0,4

b)

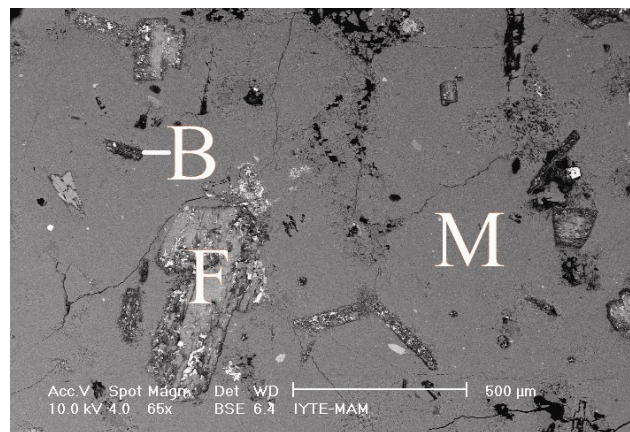
Figure 51. Graph a) and table b) showing the amounts of major and minor elements in unweathered andesite sample

#### 4.1.4. Microstructural and Petrographical Characteristics of Andesite

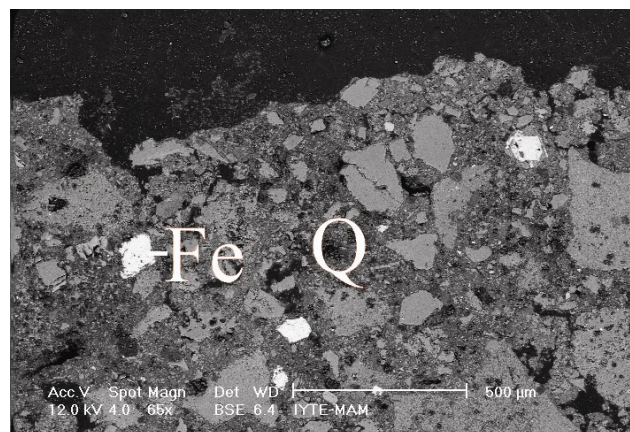
Microstructural characteristic of andesite have been determined by SEM analysis. In petrographic analysis, minerals are determined by polarized microscope analysis. In XRD analysis of the samples, the possible minerals exist in andesite were determined as andesine, albite high, anorthite, kyanite, labradorite, muscovite,

microcline, mullite, orthoclase, orthoferrosilite, quartz, sanidine and tridymite. The same minerals are observed in SEM and petrographic analysis, too.

In the SEM analysis, rectangular shape of feldspars about 300 x 500  $\mu\text{m}$  in size were observed in the volcanic matrix. Biotite minerals (about 250 $\mu\text{m}$  in length), iron (about 100 x 100 $\mu\text{m}$ ) and quartz minerals (smaller than 100 $\mu\text{m}$ ) were observed in the matrix of andesite (Figure 52). The amorphous phases were also observed in BSE images of the samples (Figure 53).



a)



b)

M: Matrix, B: Biotite, F: Feldspar, Fe: Iron, Q: Quartz

Figure 52. BSE images of feldspar, biotite a), iron and quartz b) in the matrix of andesite sample

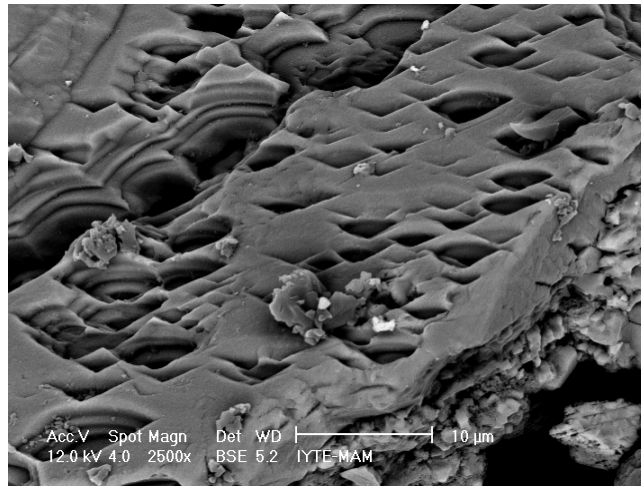
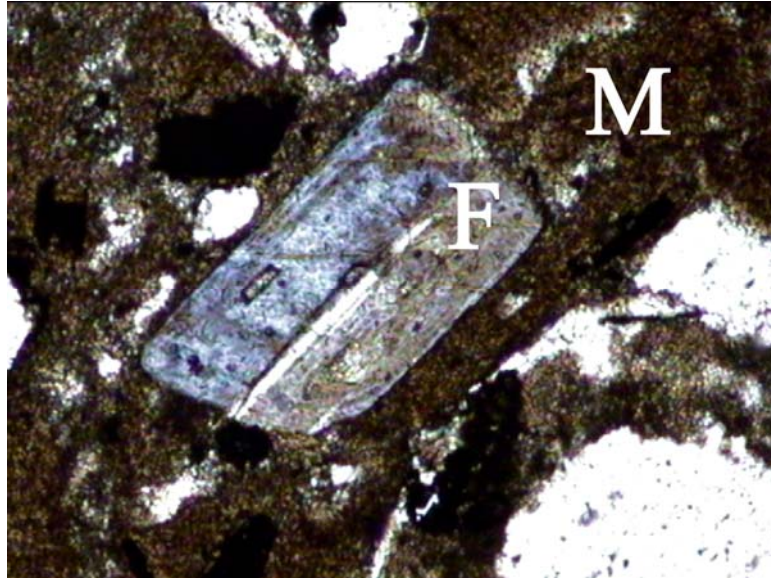
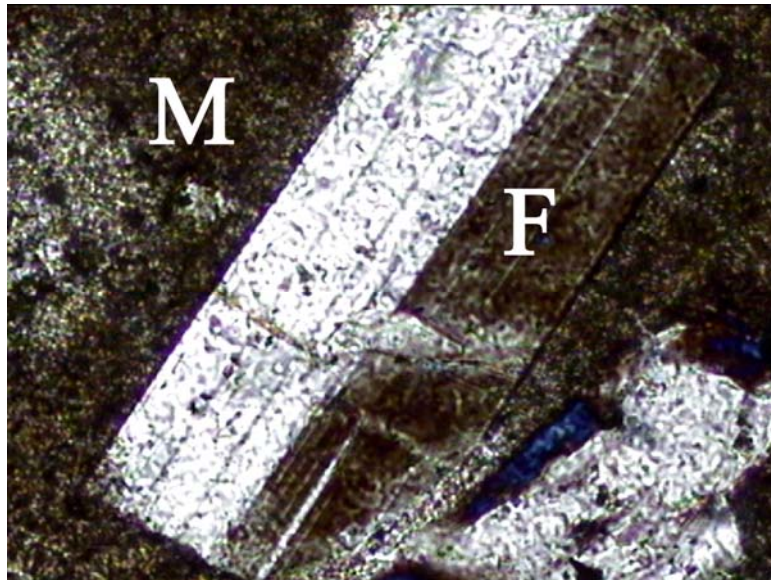


Figure 53. BSE image showing the amorphous phases in the composition of andesite

In petrographic analysis, feldspar twins, biotite and quartz were mainly observed in the volcanic matrix (Figure 54).



a)

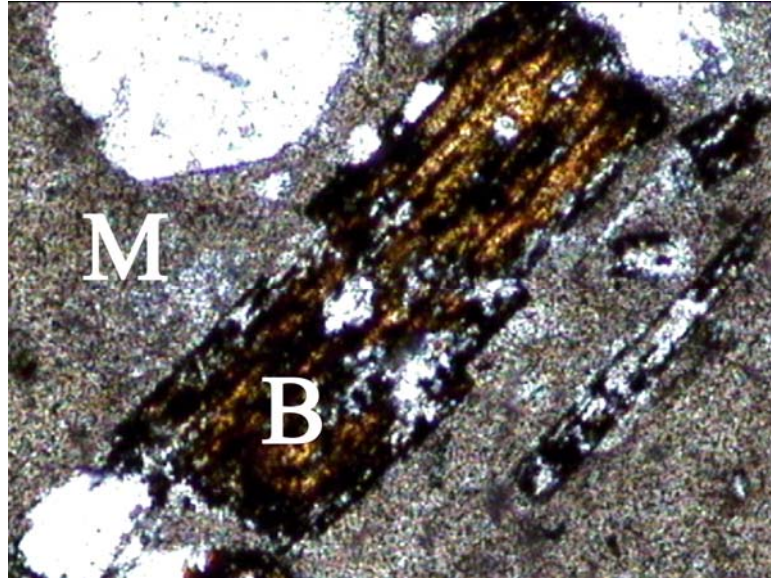


b)

M: Matrix, F: Feldspar, B: Biotite

Figure 54. Thin section images of feldspar a), b) and biotite minerals c) in the matrix of sound andesite sample x40

(cont. on next page)



c)

M: Matrix, F: Feldspar, B: Biotite

Figure 54. (cont.) Thin section images of feldspar a), b) and biotite minerals c) in the matrix of sound andesite sample x40

#### 4.1.5. Weight Loss of Andesite by Thermogravimetric Analysis

Amount of clay minerals and organic materials of the stone have been determined by TGA analysis. The total weight loss is a negligible value.

The weight losses were observed in the range of 25-103 °C due to absorbed water and 103-550 °C due to decomposition of clay minerals and organic materials respectively (Figure 55). The increase observed between 600 and 1000 °C can be explained by the oxidation of iron compounds of andesite (Pansu and Goutheyrou 2006).

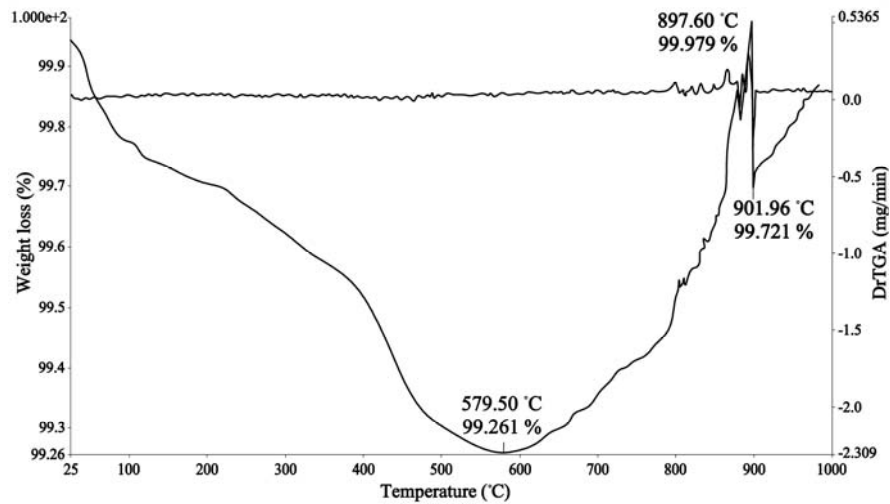


Figure 55. TGA graph of the sound andesite sample from the inner part of the stone

## 4.2. Characterization of Infill Material in the Rubble Core of the Wall

Infill material was used to strengthen and stabilize the inner core of the wall of the building structurally. In order to stabilize the wall section itself, the weight of the wall is increased by raising the wall or splaying out the base of the wall (Bonde, et al. 1995). In agora, the wall was strengthened by mixing of soil and pebble stone. In this study, material characteristics of soil fraction of the infill materials was determined. In this part of the study, basic physical properties, mineralogical characteristics and chemical compositions of soil fractions used as a part of infill material were expressed and discussed.

### 4.2.1. Particle Size Distribution of Infill Material

Particle size distribution of soil used in infill was determined by sieve analysis (Teutonico 1988). Aggregates with particle size of 1180  $\mu\text{m}$  composed the largest fraction of soil particles with the range of 29 %. Each of the particles in the sizes of

500-1180  $\mu\text{m}$  and 250-500  $\mu\text{m}$  composed 18 %. Aggregates with particle size of 125-250  $\mu\text{m}$  composed 24 % of the whole soil. Aggregates smaller than 125 $\mu\text{m}$  composed the smallest fraction with the range of 10 % (Figure 56). Results of sieve analysis showed that the soil used in the rubble core was mostly composed of fine aggregates (less than 1 mm) with the total range of 70 %. The aggregates existed in the soil are semi-circular in shape and light or dark grey in color (Figure 57).

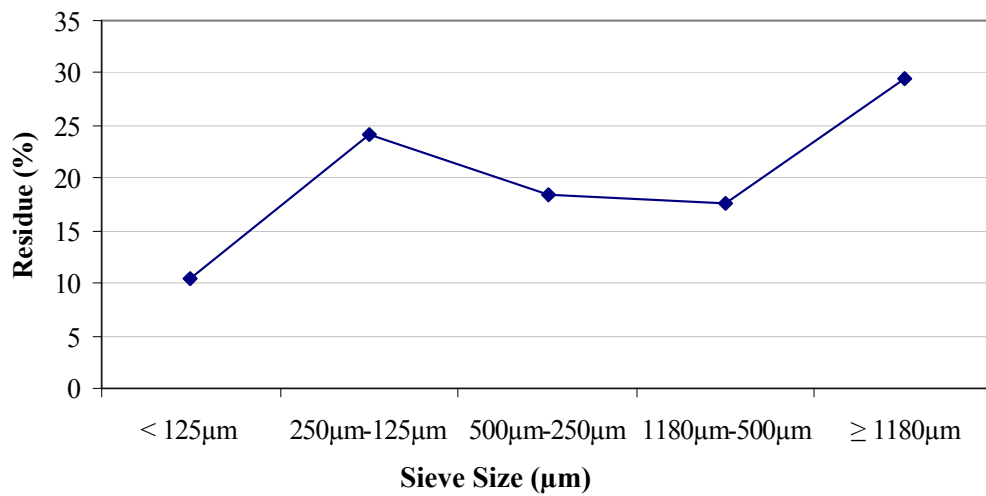


Figure 56. Particle size distribution of aggregates of soil used as infill material in the rubble core

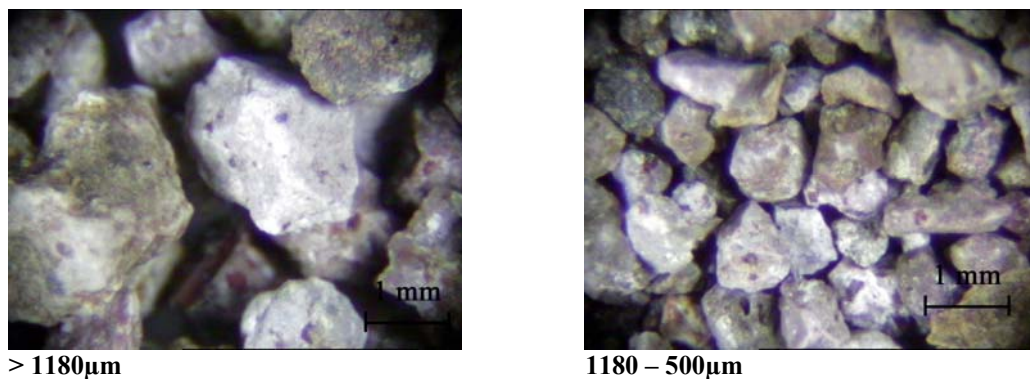


Figure 57. Stereo microscope images of aggregates in the soil used as infill material in the rubble core

(cont. on next page)



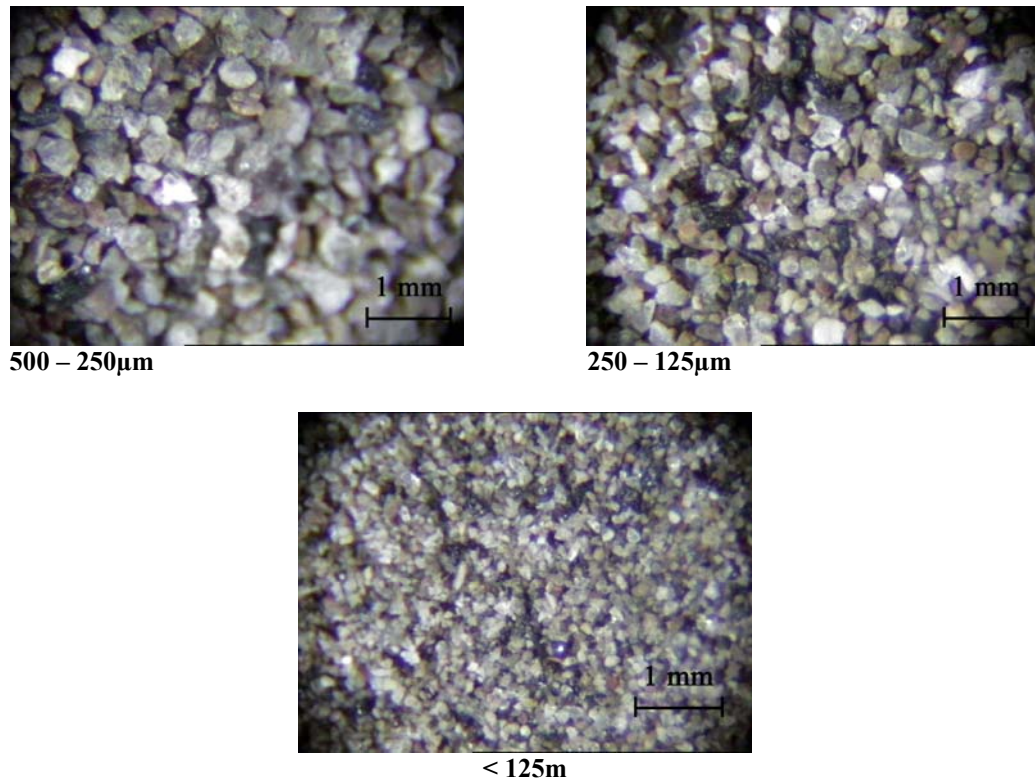
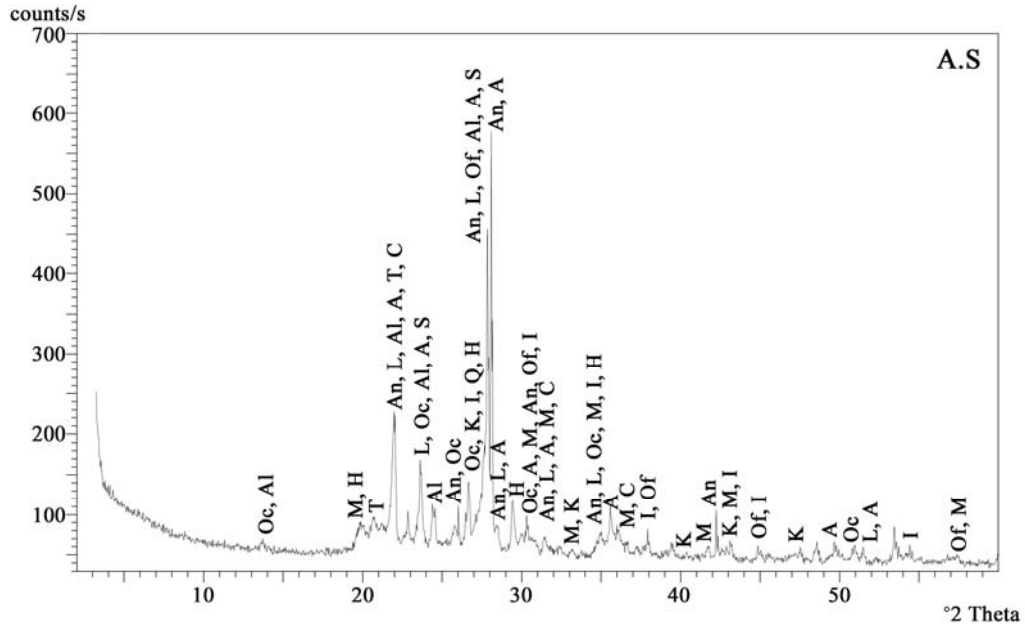


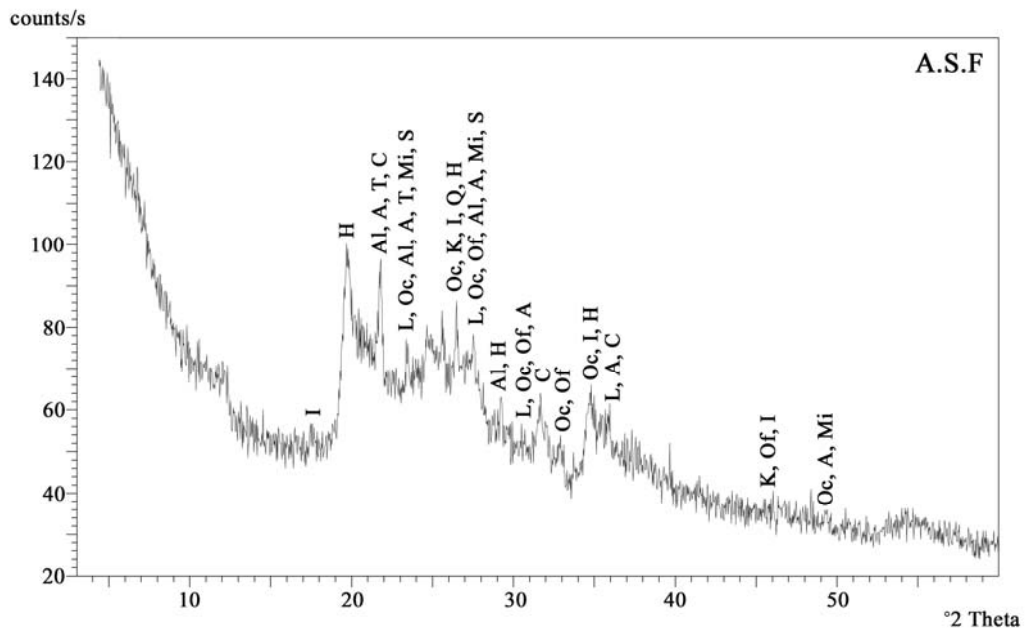
Figure 57. Stereo microscope images of aggregates in the soil used as infill material in the rubble core

#### 4.2.2. Mineralogical Composition of Soil Fraction in the Infill Material

Mineralogical composition of soil and its fraction less than 53 microns were determined by XRD and FT-IR analysis. Mineralogical analysis carried out by XRD show that they were composed of andesine, albite high, anorthite, cristobalite, halloysite, illite, kyanite, labradorite, microcline, mullite, orthoclase, orthoferrosilite, quartz, sanidine, tridymite and calcite (Figure 58). They were also determined by FTIR analysis. The IR spectrums of both samples had similar IR spectrums (Figure 59). In their IR spectrums, O-H stretching vibrations are in the range of  $3700\text{--}3200\text{ cm}^{-1}$  and Si-O stretching is at around  $1050\text{ cm}^{-1}$ . Quartz ( $795\text{--}792\text{ cm}^{-1}$ ,  $695\text{ cm}^{-1}$ ,  $538\text{ cm}^{-1}$  and  $470\text{ cm}^{-1}$ ), calcite ( $1436\text{ cm}^{-1}$ ,  $876\text{ cm}^{-1}$  and  $712\text{ cm}^{-1}$ ), and hematite ( $538\text{ cm}^{-1}$  and  $470\text{ cm}^{-1}$ ) minerals were also identified in the IR spectrums. The presence of calcite minerals may show that soil fraction of infill materials is not obtained from the andesite quarries.



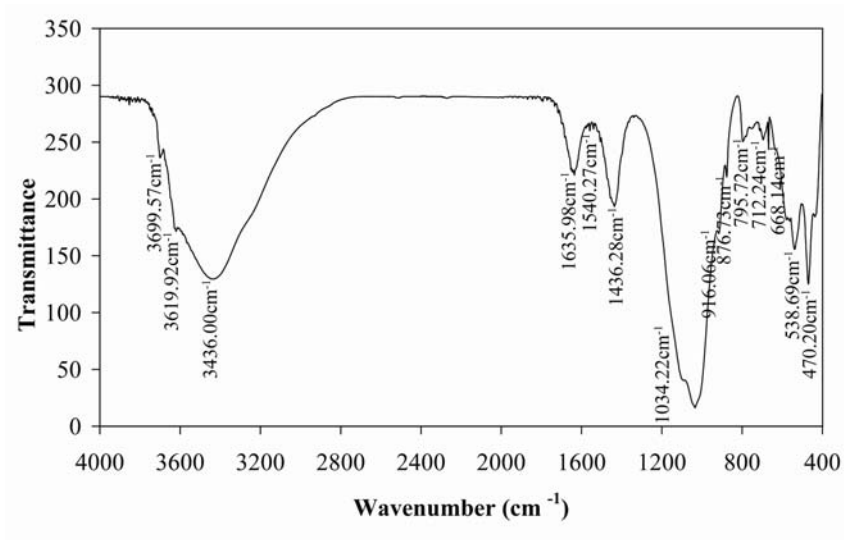
a)



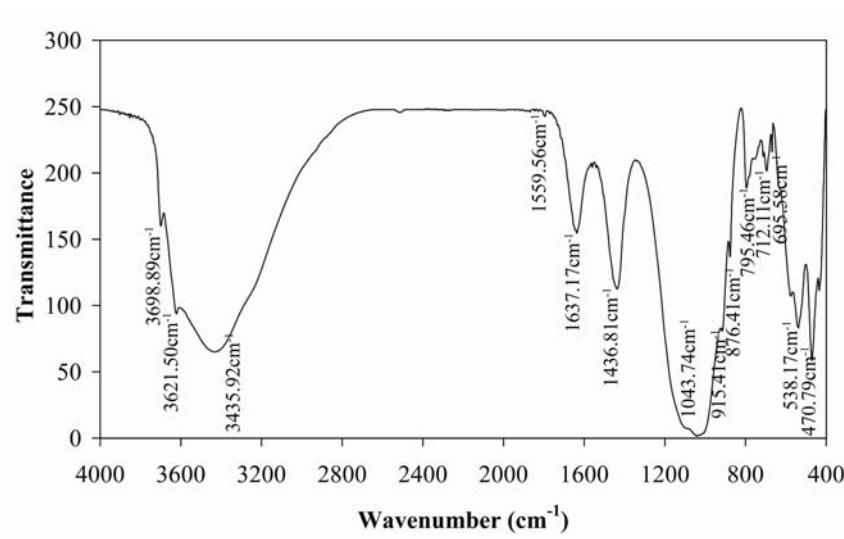
b)

A: Andesine (79-1148), Al: Albite high (83-1608), An: Anorthite (70-0287), C: Cristobalite (82-1403), H: Halloysite (03-0184), I: Illite (15-0603), K: Kyanite (72-1441), L: Labradorite (83-1368), Mi: Microcline (76-1238), Mu: Mullite (02-1160), Oc: Orthoclase (75-1190), Of: Orthoferrosilite (83-0668), Q: Quartz (83-2468), S: Sanidine (19-1227), T: Tridymite (42-1401)

Figure 58. XRD patterns of soil sample a) and soil fraction less than 53  $\mu\text{m}$  b)



a)



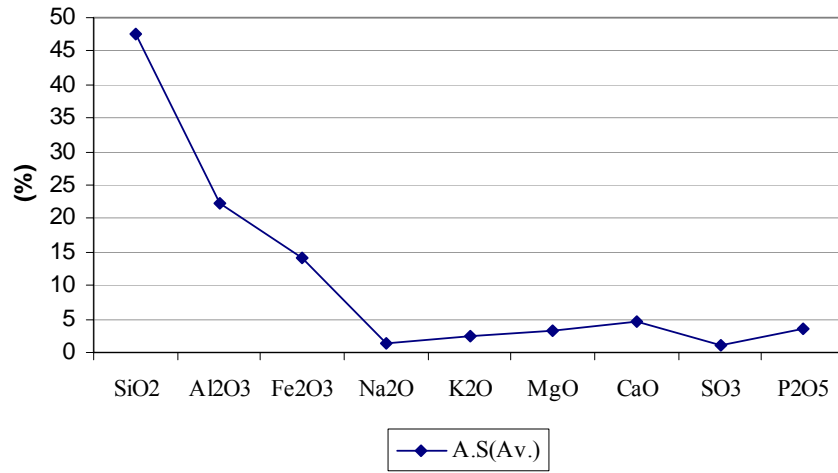
b)

Figure 59. FT-IR graphs of soil sample a) and soil fraction less than 53  $\mu\text{m}$  b) taken from infill

### 4.2.3. Chemical Composition of Soil Fraction in the Infill Material

Chemical composition of soil fraction was determined by SEM-EDS analysis. Silicon dioxide ( $\text{SiO}_2$ ), aluminum oxide ( $\text{Al}_2\text{O}_3$ ) and iron oxides ( $\text{Fe}_2\text{O}_3$ ) were determined as the major oxides. The minor oxides were sodium oxide ( $\text{Na}_2\text{O}$ ),

potassium oxide (K<sub>2</sub>O), magnesium oxide (MgO), calcium oxide (CaO), sulphur trioxide (SO<sub>3</sub>) and phosphorus pentoxide (P<sub>2</sub>O<sub>5</sub>) (Figure 60).



a)

Sample	SiO <sub>2</sub>	Al <sub>2</sub> O <sub>3</sub>	Fe <sub>2</sub> O <sub>3</sub>	Na <sub>2</sub> O	K <sub>2</sub> O	MgO	CaO	SO <sub>3</sub>	P <sub>2</sub> O <sub>5</sub>
A.S(1)	42.69	20.88	15.91	2.29	2.69	3.89	4.98	2.39	4.27
A.S(2)	50.33	23.06	13.35	1.16	1.87	2.85	4.56	0	2.83
A.S(3)	49.68	23.04	12.78	0.89	2.53	2.87	4.35	0.79	3.08
A.S(Av.)	47.6 ± 4.2	22.3 ± 1.3	14.0 ± 1.7	1.4 ± 0.7	2.4 ± 0.4	3.2 ± 0.6	4.6 ± 0.3	1.1 ± 1.2	3.4 ± 0.8

b)

Figure 60. Graph a) and table b) showing the amounts of major and minor elements in soil taken from infill

#### 4.2.4. Weight Loss of Soil Fractions by Thermogravimetric Analysis

The approximate amount of clay, organic materials and carbonate content in the the soil fraction less than 53 µm was determined by TGA analysis. The total weight loss of infill material is 19.38 %. The weight losses in infill material are 3.32 % due to absorbed water, 13.9 % due to decomposition of clay minerals and organic materials and 2.16 % due to CO<sub>2</sub> content. (Figure 61). The results may show the use of higher

amounts of clays in the composition of infill material due to binding properties of clay minerals.

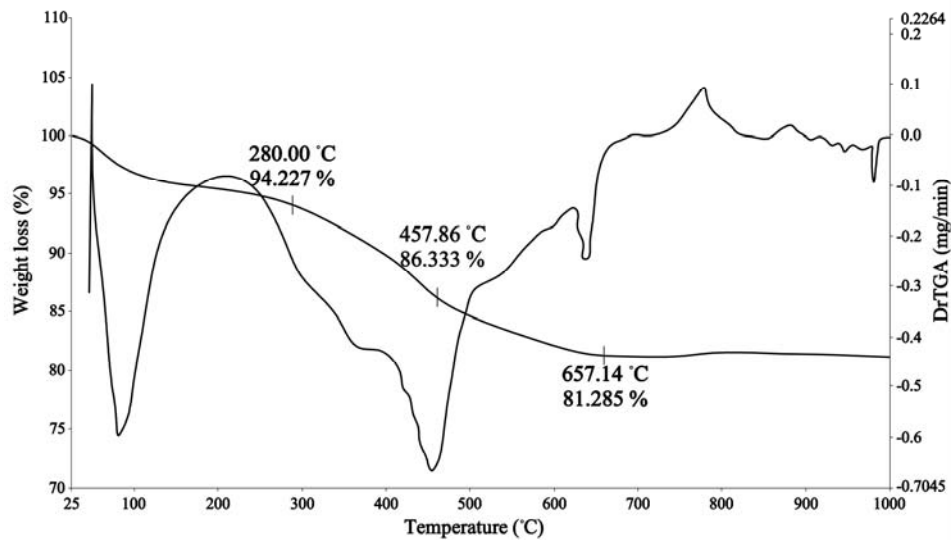


Figure 61. TGA graph of soil fraction less than 53  $\mu\text{m}$  taken from soil infill

### 4.3. Main Causes of Weathering of Andesite

In this part of the study, the possible causes of the weathering observed on the building stones are expressed and discussed considering the experimental study results.

Changes of porosity values and difference in mineralogical and chemical compositions from the exterior surface to their inner parts of the stone are the main characteristics of the weathering.

The main causes of weathering observed on andesite can be defined in four main headings as follows:

- Effects of climatic conditions
- Effects of clay minerals
- Effects of biological growth
- Effects of salt crystallization

### **4.3.1. Effects of Climatic Conditions on the Weathering of Andesite**

Climatic condition of the site is the main factor of the physical and chemical weathering of andesite. Condensation occurs mostly in winter months (Figure 14) with increasing relative humidity (Oxley and Gobert 1985). In winter months, frosty days (approximately 21 days in winter) accelerate the physical weathering of the stone. The water condensed in the pores of the stone expands with freezing. It causes micro-cracks and fissures (Schaffer 1932). High rainfall is observed in winter months (Figure 13). Hence, November, December, January and February seem to be the most effective months in a year for the weathering of andesite used in the construction of the agora.

#### **Effects of climate on the basic physical properties of the andesite**

Increase of porosity and decrease of density values of the stone from its inner part to its exterior surface is the main characteristics of the physical weathering. In this study, density and porosity values of sound and weathered stone samples were determined by standard test methods (RILEM 1980). Density and porosity values of sound andesite were about 2.4 g/cm<sup>3</sup> and 8 %. The density values decrease to 2.0 g/cm<sup>3</sup> and porosity varies between 14.6 % and 21.5 % in weathered parts of the stone.

The changes in porosity were observed in detail from the BSE images of the samples which were cut perpendicular to the stone surface, as well. The porosity increases from inner parts to the exterior surface of the stone (Figure 62). The increase in porosity causes physical disintegration and loss of stone material on the surfaces of building stones. The increase in porosity of the stone also causes the reduction in strength and increase in deformability (Arıkan, et al. 2007).

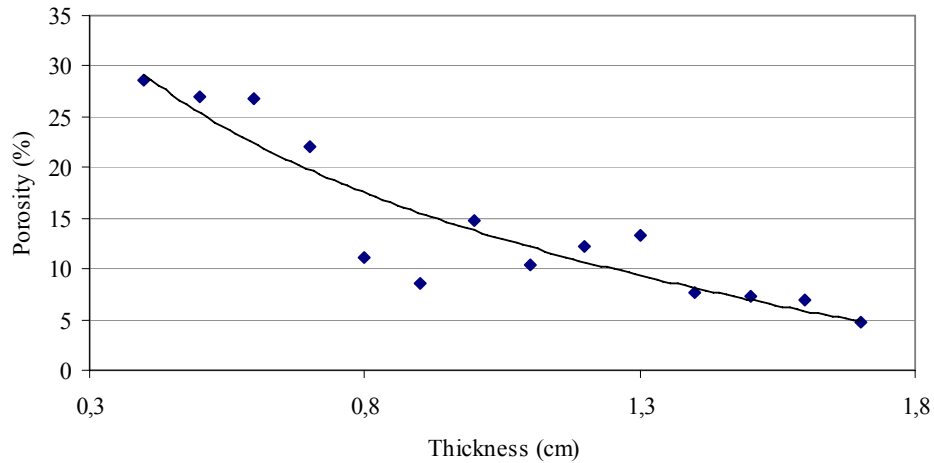


Figure 62. Porosity change from exterior surface to sound inner parts of the stone

The porosity values determined from BSE images can be used to determine the weathering rate of stone per year using the formula below (Friedman and Long 1976).

$$L = (D \cdot t)^{1/2} = D^{1/2} \cdot t^{1/2}$$

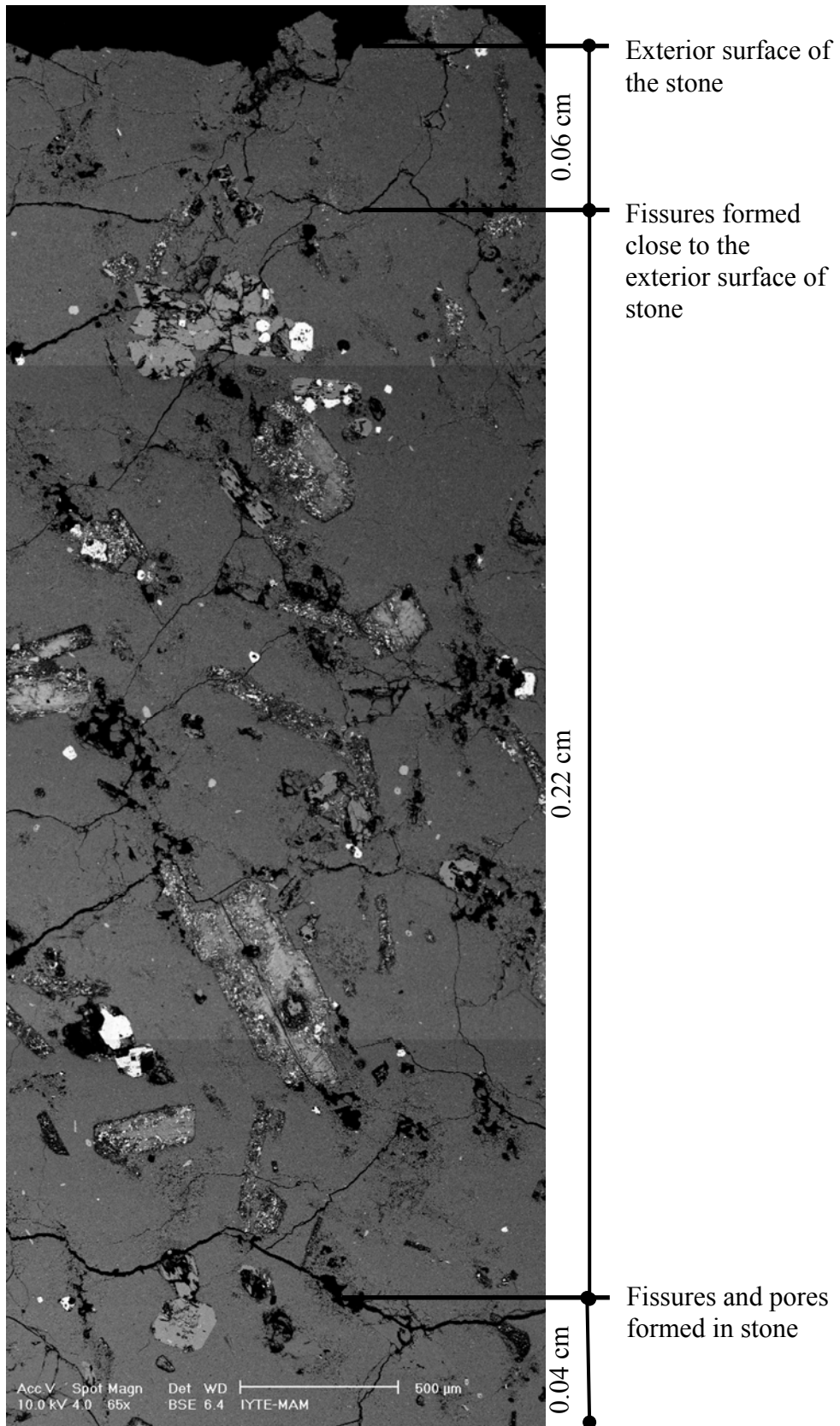
where;

L: Thickness of the weathered zone (mm)

D: Diffusion coefficient (mm<sup>2</sup>/year)

t: year

The “L” value was about 1.7 cm for andesite used in agora, considering the data taken from BSE images (Figure 63). The “t” value was considered as the the age of the building which is about 2300 years because of cut-stone use on the facade. The results show that the rate of weathering of andesite is approximately 0.125 mm<sup>2</sup> per year. In the study of Oguchi and Matsukura, the weathering rate of andesite samples collected from the terraces of Nasuna-ga-hara was calculated using the same equations (Oguchi and Matsukura 1999). However, the age of the stones in Nasuna-ga-hara were calculated considering the first formations of the stones. Additionally, the samples were taken from 2.0 m under tephra layer. Considering all these differences, the weathering rate of Aigai andesite is normally higher than Nasuna-ga-hara andesites.

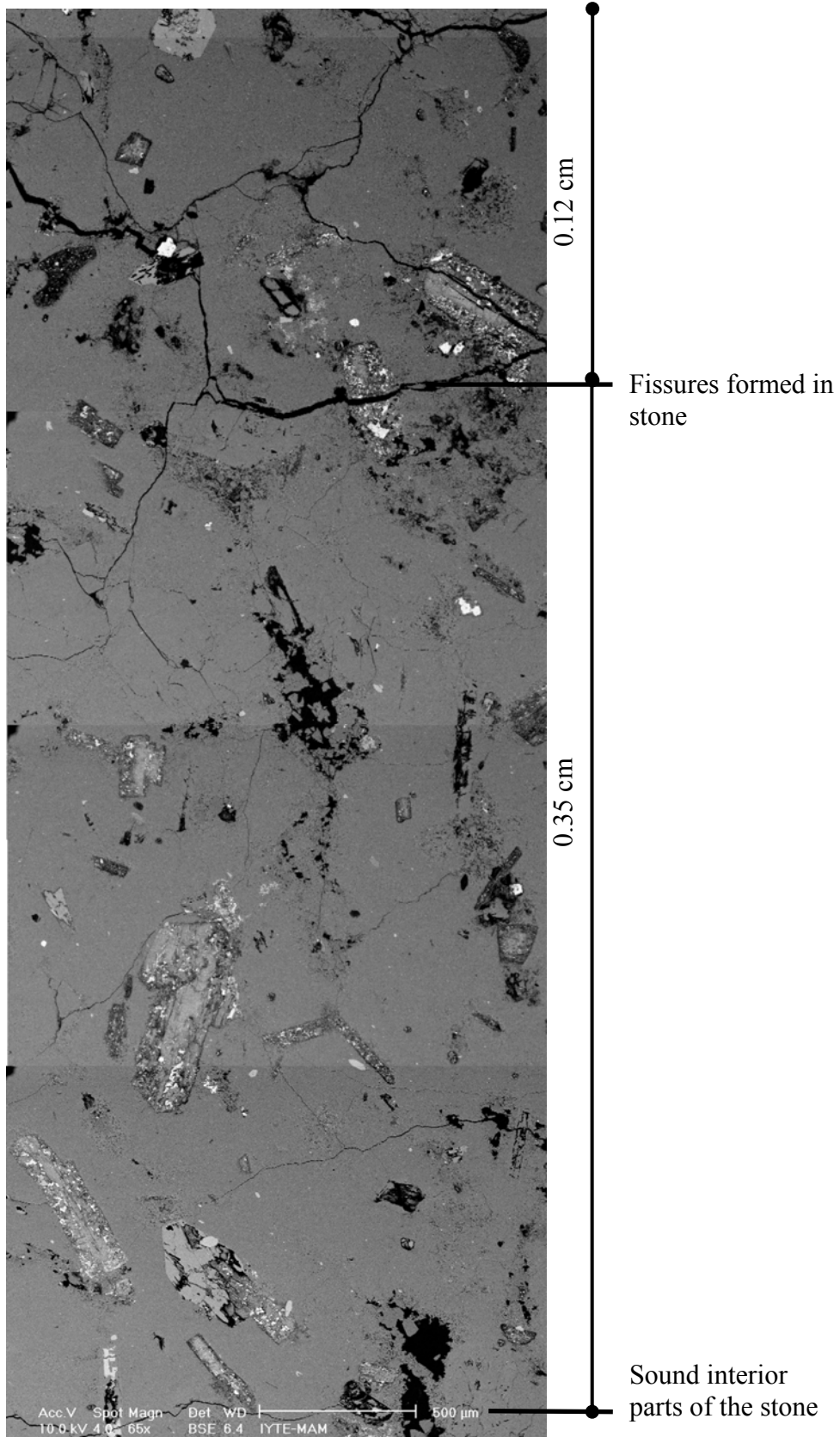


a)

Figure 63. BSE image of crack formation from exterior surface a) to the sound inner parts b) of the stone

(cont.on next page)





b)

Figure 63. (cont.) BSE image of crack formation from exterior surface a) to the sound inner parts b) of the stone

## Effects of climate on the mineralogical and chemical compositions of the andesite

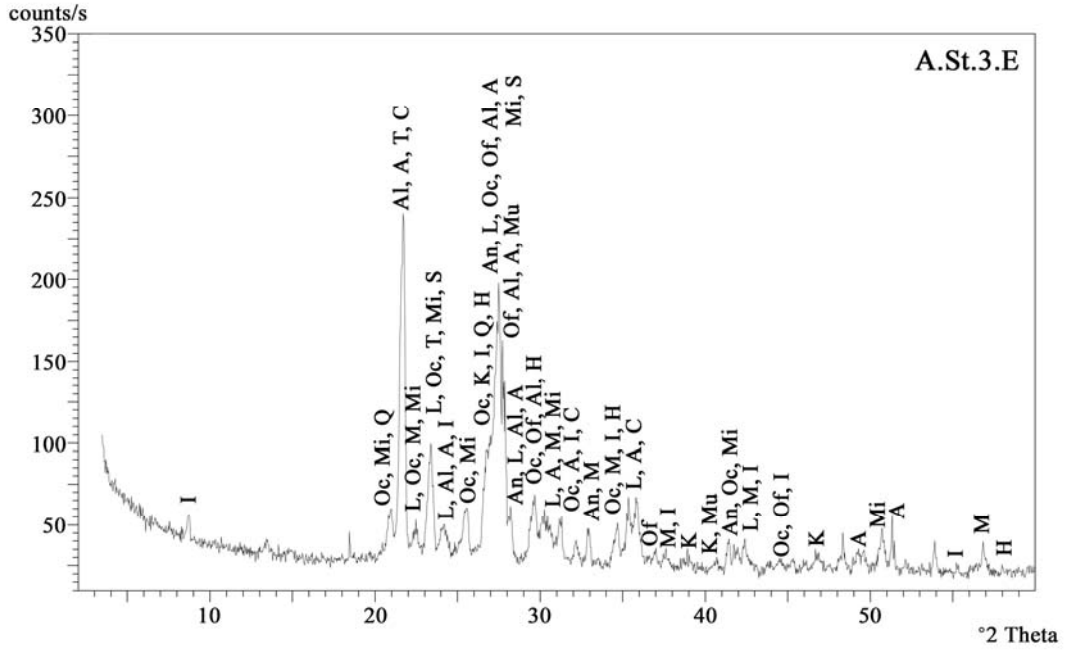
Mineralogical and chemical compositions of unweathered and weathered andesites samples have been determined by XRD, FT-IR and SEM – EDS analysis in order to indicate the effects of climate on the weathering process.

XRD analysis results of the unweathered samples showed that they were mainly composed of andesine, albite high, anorthite, kyanite, labradorite, muscovite, microcline, mullite, orthoclase, orthoferrosilite, quartz, sanidine and tridymite. But, clay minerals were indicated on the exterior and inner crack surfaces of the stone (Figure 64).

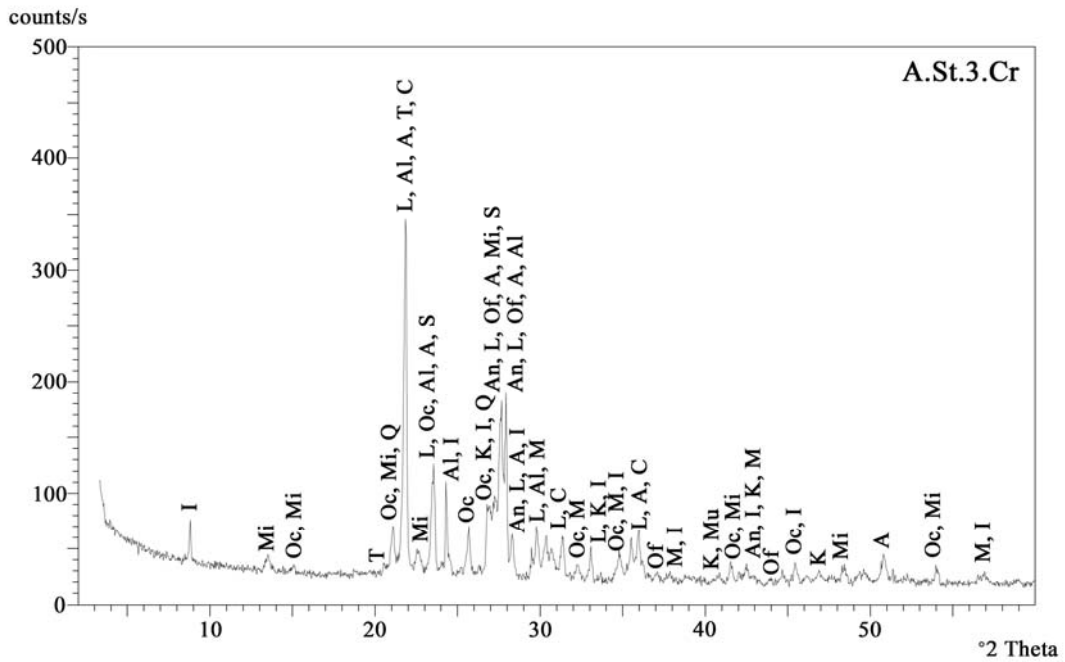
In the IR spectrum of samples taken from exterior and inner crack surface of the stone, O-H stretching vibrations are observed in the range of  $3700-3200\text{ cm}^{-1}$ , Si-O stretching at around  $1090\text{ cm}^{-1}$  and Fe-O stretching at  $470\text{ cm}^{-1}$  (Figure 65). The presence of clay minerals and iron oxide compounds may show the chemical weathering of andesite with water and carbon dioxide.

The elemental composition analysis results showed that the amount of  $\text{SiO}_2$  varied between the ranges of 50 % and 60 % in the unweathered and weathered andesite (Figure 66). On the exterior surface of the weathered andesite, the amount of  $\text{Fe}_2\text{O}_3$  increases comparing with the sound inner parts. The  $\text{Fe}_2\text{O}_3$  content varies between 7 % and 15 % in the sound parts while it reaches to 26 % in weathered stone sample.

High amounts of iron compounds on the weathered surfaces can be explained by the effects of water. When the exterior surface gets wet, the water penetrates from exterior surface to the inner parts of the stone. In the interior, hematite is dissolved and mobilized by water. When the exterior surface is dry, the water movement is reversed.  $\text{Fe}^{2+}$  is moved to the dry surfaces by water and oxidized to form  $\text{Fe}^{3+}$ . As a result,  $\text{Fe}_2\text{O}_3$  is formed on the exterior surfaces (Oguchi 2001).



a)



b)

Figure 64. XRD patterns of weathered andesite samples taken from the exterior surface a) and inner crack surface of the stone b)

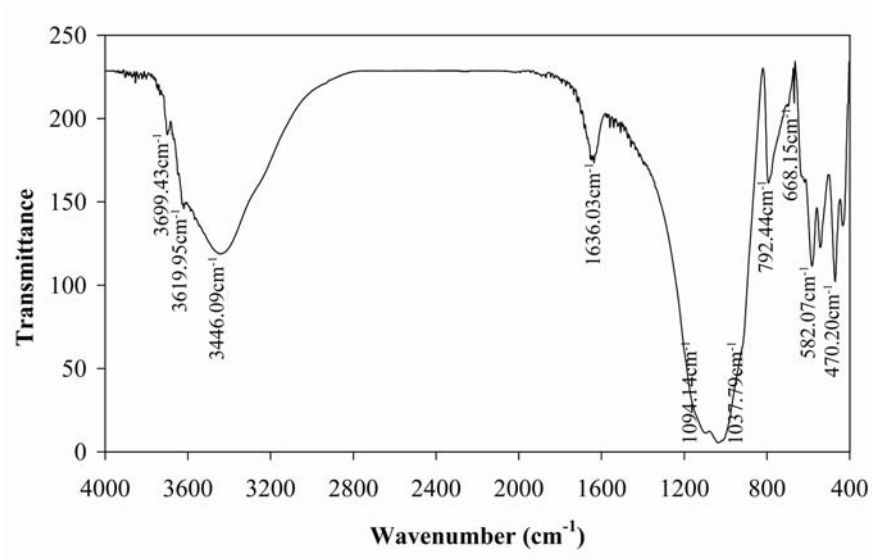


Figure 65. FT-IR spectrum of samples taken from inner crack surface of the stone

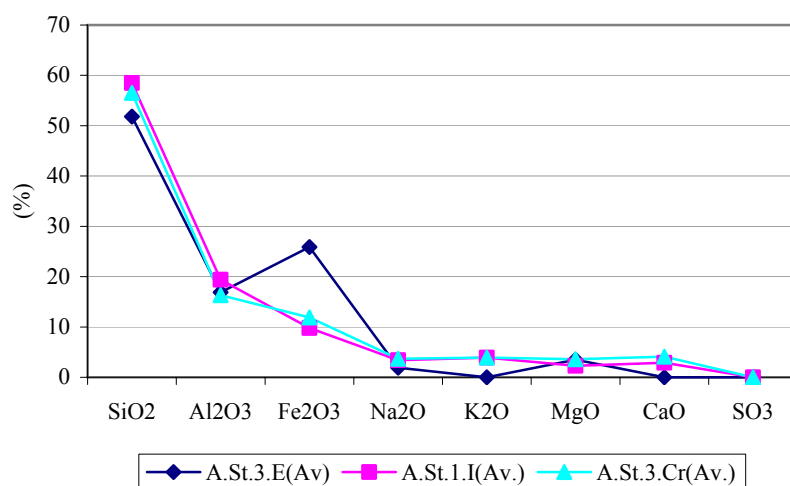


Figure 66. Elemental compositions of unweathered and weathered stone samples

### 4.3.2. Effects of Clay Minerals on the Weathering of Andesite

The existence of clays on the exterior and the interior parts of the stone accelerates its weathering by swelling and providing the formation of algae, lichen, moss, etc. (Press and Siever 2002). Clays expand in moist environment and cause the

formation of fissures and cracks in stone (Scherer 2006). Due to porous characteristic of andesite, rainwater and condense water penetrate through the inner parts of the stone and cause the expansion of clay minerals (Figure 67).

Clay minerals and iron oxide compounds were determined in the samples by XRD and FT-IR analysis taken from exterior and inner crack surfaces of the stone (Figure 64, Figure 65). They were also indicated in the SEM analysis of the samples taken from exterior surfaces and inner cracks surfaces (Figure 68).

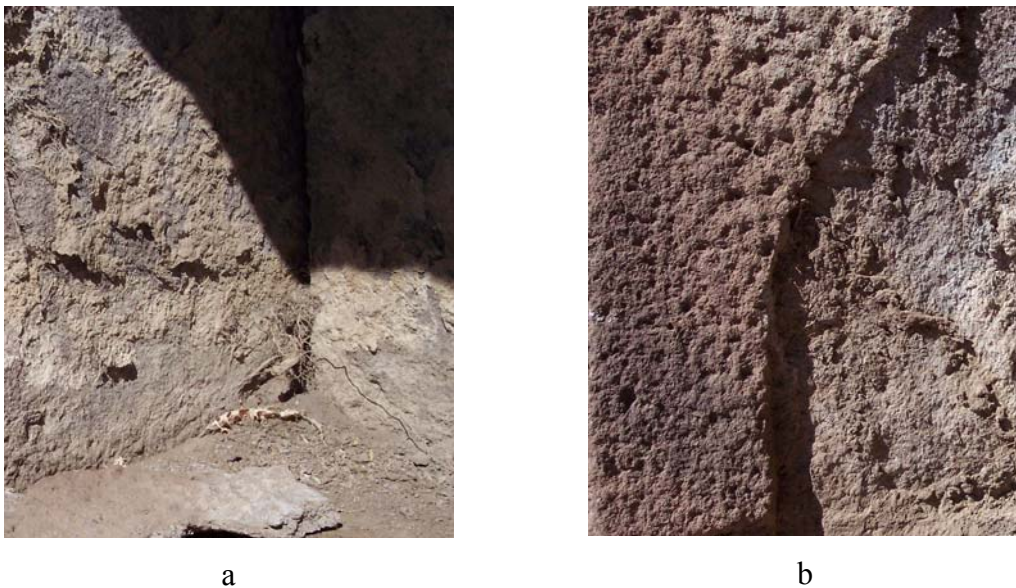


Figure 67. Scaling as a result of clay formation inside of the stone

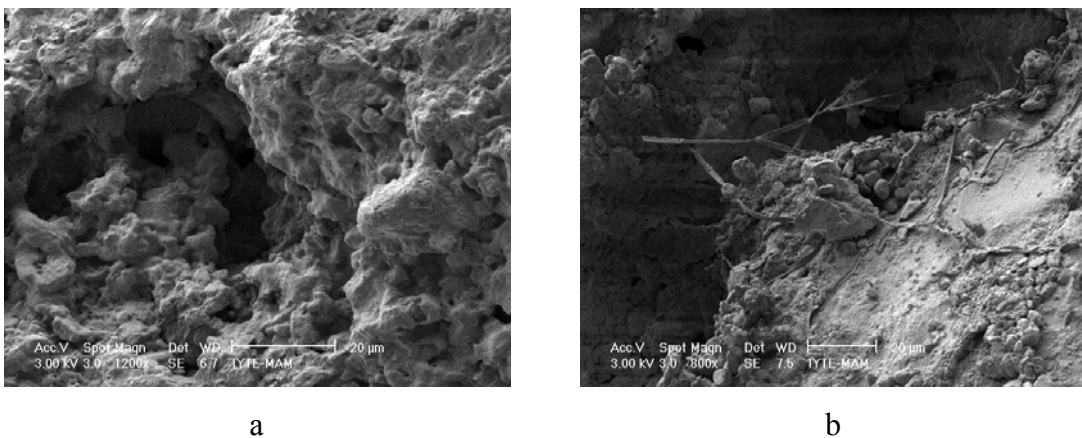


Figure 68. SE images of clay deposition on the exterior a) and inner crack surfaces with microbiological growth b)

### 4.3.3. Effects of Biological Growth on the Weathering of Andesite

Clay minerals not only develop swelling pressures but also provide the environment for biological growth (Press and Siever 2002). On the stone surfaces of agora, clays and microbiological growth were observed together. The disintegration of the stone occur by hypal penetration, expansion and contraction, freeze and thaw of thallus, swelling action of organic or inorganic salts originated from biological growth such as lichens, algae, mosses, etc. (Chen, et al. 1999). The effect of respiratory CO<sub>2</sub>, mineral dissolution by excretion of organic acid, and other possible mechanisms such as metabolic and enzymatic reactions are the chemical effects of biological growth on the stone (Chen, et al. 1999).

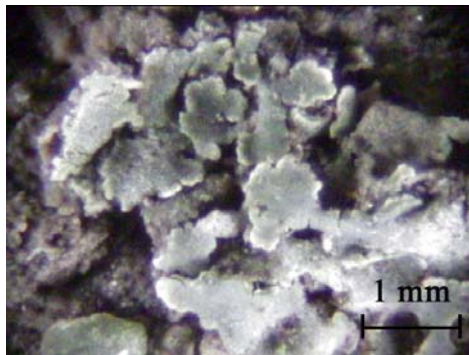
Biological growth is observed on the whole facade by naked eye on the upper parts of the southeast wall (Figure 69) and on the northeast wall of the building (Figure 70). SEM-EDS analysis indicated that they contain high amounts of carbon and oxygen and low amounts of Al and silicon. The presence of Al and Si may show the existence of clay minerals (Figure 71).



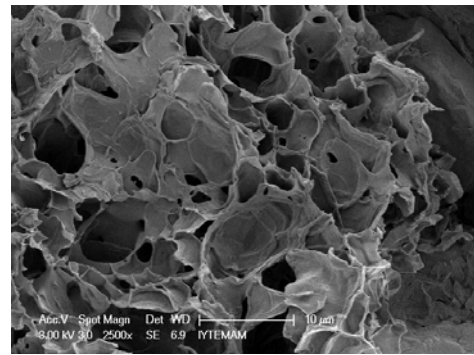
Figure 69. Lichen colonization on the upper parts of the wall



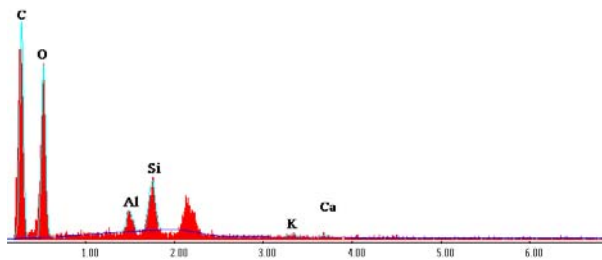
Figure 70. Lichen colonization on the northeast facade of the building



a)



b)



c)

<u>Element</u>	<u>%</u>
C	54.04
O	32.80
Al	3.31
Si	7.65
K	1.43
Ca	0.78
<b>Total</b>	<b>100.00</b>

d)

Figure 71. Optic microscope image a), SE image b), EDX spectrum c) and chemical composition d) of lichens taken from the exterior surface of andesite

#### 4.3.4. Effect of Salt Crystallization on the Weathering of Andesite

Stones are weathered by soluble salts through crystallization and hydration reactions (Schaffer 1932). The efflorescences were not visible on the exterior surface of the wall except the lintels of the chamber entrances and windows, and northern part of the facade.

In this study, the soluble salt contents of the exterior stone and soil samples were determined to estimate the salt weathering effects on the stone. The minor amounts of soluble salts less than 0.5 percent were found in the stone and soil samples (Figure 72).  $\text{NO}_2^-$ ,  $\text{NO}_3^-$ ,  $\text{SO}_4^{=}$  and  $\text{Cl}^-$  ions were not detected in any of the soil or stone samples. However,  $\text{PO}_4^-$  ions were observed in one of the exterior surfaces and in soil.

Visible efflorescence was observed on the surface of the lintels of each chamber door and window openings, and northern part of the facade (A.Eff.1) (Figure 73). Its mineralogical and chemical composition were determined by FT-IR and SEM-EDS analysis. The elemental composition analysis of efflorescence indicated that it mainly consisted of  $\text{SO}_3$  and  $\text{CaO}$  (Figure 74).

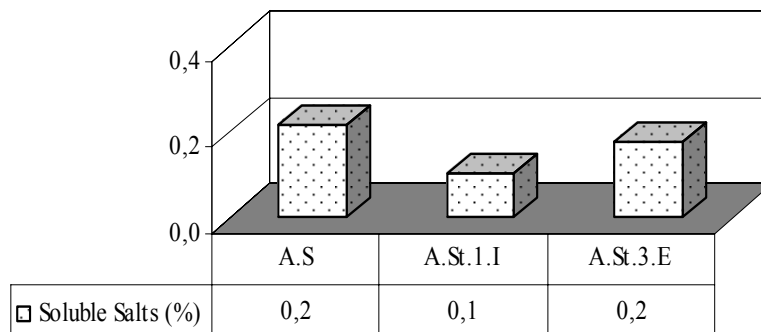
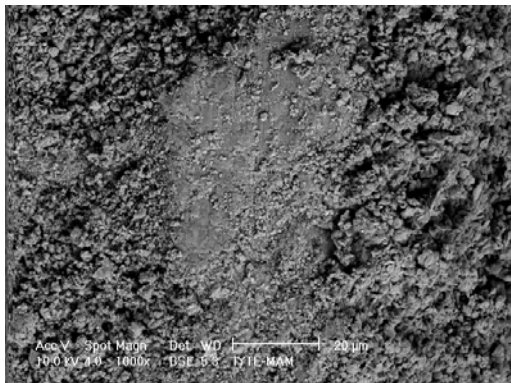


Figure 72. Soluble salt content of unweathered and weathered andesite and infill material

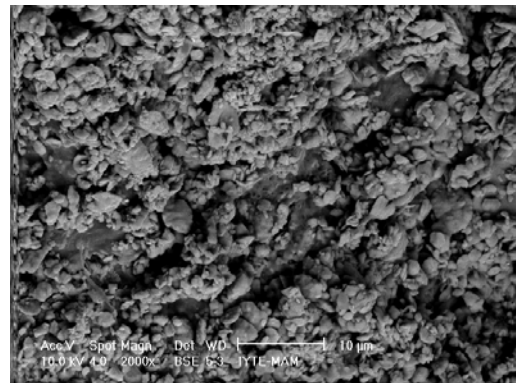




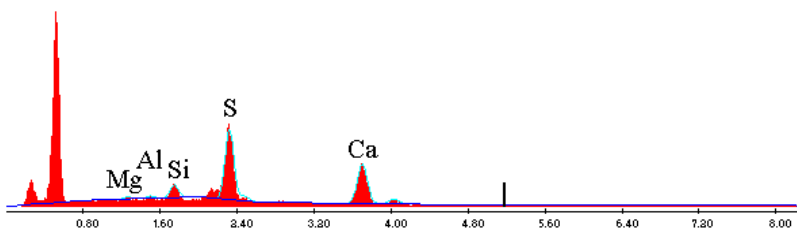
Figure 73. Efflorescence on the surfaces of vertical and horizontal stone blocks defining the entrance to the 7th interior chamber



a)



b)



c)

<b>Element</b>	<b>%</b>
MgO	0.70
Al <sub>2</sub> O <sub>3</sub>	0.82
SiO <sub>2</sub>	6.20
SO <sub>3</sub>	53.62
CaO	38.65
<b>Total</b>	<b>100.00</b>

d)

Figure 74. BSE images a), b), EDX spectrum c) and chemical composition d) of efflorescence taken from the surface of the stone of horizontal lintel, A.Eff.1

In its IR spectrum, vibration bands due to the hydrated sulphate (Gypsum -  $\text{CaSO}_4 \cdot 2\text{H}_2\text{O}$ ) was observed at  $3560 \text{ cm}^{-1}$ ,  $1685 \text{ cm}^{-1}$ ,  $1621 \text{ cm}^{-1}$ ,  $1622 \text{ cm}^{-1}$ ,  $1117 \text{ cm}^{-1}$ ,  $672 \text{ cm}^{-1}$ ,  $601 \text{ cm}^{-1}$  and  $472 \text{ cm}^{-1}$  (Figure 75). These results showed that efflorescence was mainly composed of gypsum.

Gypsum has been used as a building material for different purposes such as plastering, decoration etc. It is also observed on calcareous stones as a results of the reaction of  $\text{SO}_2$  with calcium carbonate in the presence of water (Böke 2003). The stone of agora is andesite and the site is located in a suburban area away from air pollution. So, it is difficult to explain the reasons of its use and the date of the application.

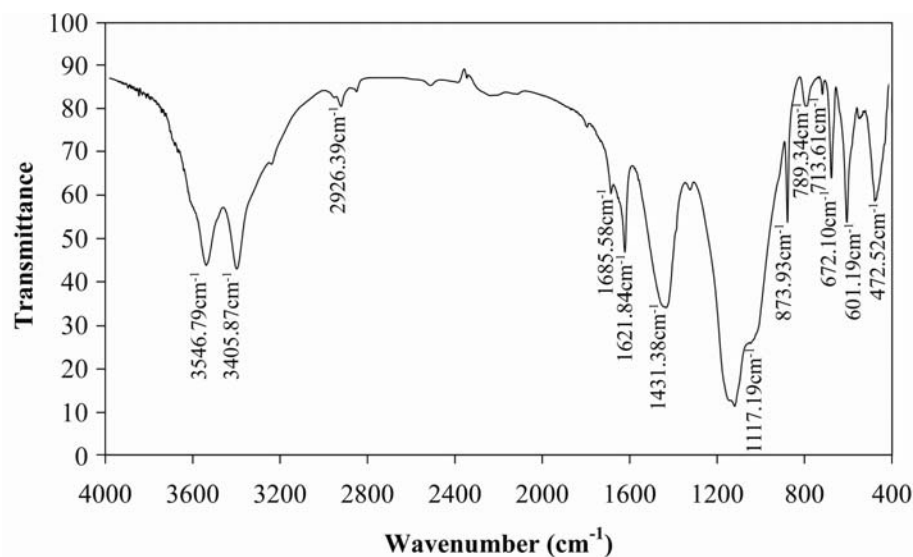


Figure 75. FT-IR spectrum of efflorescence taken from the surface of the stone of the horizontal lintel

## CHAPTER 5

### CONCLUSION

The aim of this study was to determine the construction technique, material characteristics and deterioration problems observed on the southeast facade of Aigai Agora for the purpose of its conservation.

Aigai Agora was a three storied masonry building before collapsing partially. Today, southeast facade, ground floor and some parts of the upper floors still exist. In the construction of the walls, three sections are observed: outer and inner facings with cut-stone, and rubble core. Infill material of the rubble core is composed of soil and pebble stones. Its soil fraction is mostly composed of fine aggregates (less than 1 mm) with the total range of 70 %.

In the construction of the walls, the cut-stones were used in different directions in a row and the inner and outer facings were integrated to the rubble core. Levelling course was used in three rows by the use of cut stones with different dimensions laterally.

The stone used in the construction of Agora is andesite. Andesite is composed of andesine, albite, high, anorthite, illite, kyanite, labradorite, muscovite, microcline, mullite, orthoclase, orthoferrosilite, quartz, sanidine and tridymite. It is composed mainly of silicon dioxide, aluminum oxide and iron oxide. It has a high density ( $2.4 \text{ g/cm}^3$ ) and a low porosity (8 %).

Andesite used in the construction of the building has been affected from the atmospheric conditions for nearly 2300 years. The weathering layer is about 1.7 cm on the exterior surfaces of andesite. The weathering forms observed on stone surface are mainly detachment, deposit, and loss of stone material.

Condensation and frost occurs mostly in winter months with increasing relative humidity. Humid and rainy conditions of winter months promote the physical and chemical weathering of the stone. Feldspars which are the main minerals of andesite react with the carbon dioxide in the presence of water, and clay minerals are formed.

The existence of clays on the exterior and the interior parts of andesite accelerates its weathering by swelling and causing biological growth. Types of microbiological colonization and their effects on the stone must be investigated in detail. Until the result of this investigation; the patinas on the stones should be protected.

The gypsum which is another deposition type should be cleaned. Higher plants grown in the joints of stone blocks should be pull out. Repairing or sealing cracks, cavities will prevent further growth.

Detachment observed in the stones in the forms of fissures and scaling should be consolidated. The method how to use the fallen stones in the chambers and in front of the building should be planned. Loss of stone material in the forms of granular disintegration, back weathering and break out should be consolidated. Andesite used in the conservation work of the walls should be compatible with the original ones.

The infill material is composed mainly of soil and pebble stone and it is easily dispersed in the water. Hence the infill materials should be protected from rain.

The reconstruction and integration of the building must be decided with a developed conservation approach. Structural problems must be determined and solved after a detailed investigation. The environmental design must be regarded as an important factor in the future works for the conservation of Agora. The site drainage systems should be investigated and improved in the site.

In this study, weathering forms observed on andesite used in the construction of Aigai Agora were investigated with their causes. For the future works, a conservation approach should be developed and the consolidation works must begin in the scope of this approach. For a fully developed conservation work, further researches must be carried on.

## REFERENCES

- Arikan, F., Ulusay, R., Aydın, N. 2007. Characterization of weathered acidic volcanic rocks and a weathering classification based on a rating system. *Springer-Verlag* 66 (4): 415-430.
- Arnold, A. 1983. Determination of Saline Minerals from Monuments. *GP News Letter* 4: 4-15.
- Bohn, R., Schuchhardt, C. 1889. *Altertümer von Aigai*. Berlin: Georg Reimer. Translated by Serttürk, O.K. and Kan, M.H.
- Bonde, S., Mark, R., Robinson, E.C. 1995. Walls and Other Vertical Elements. In *Architectural Technology up to the Scientific Revolution, The Art and Structure of Large-Scale Buildings*, ed. Mark, R., 52-138. USA: Sabon by DEKR Corporation.
- Böke, H., Gauri, K.L. 2003. Reducing Marble SO<sub>2</sub> Reaction Rate by the Application of Certain Surfactants. *Water Air and Soil Pollution* 142: 59-70.
- Black, C.A. 1965. *Methods of Soil Analysis, Part 2*. USA, Madison, Wisconsin: American Society of Agronomy.
- Charola, A.E. 2004. Stone Deterioration in Historic Buildings and Monuments, *Proceedings of the 10th International Congress on Deterioration and Conservation of Stone, June 27 - July 2, 2004*, ed. Kwiatkowski, D. and Löfvendahl, R. Sweden: ICOMOS.
- Chen, J., Blume, H.P., Beyer, L. 2000. Weathering of rocks induced by lichen colonization. *Catena* 39 (2): 121-146.
- Dinsmoor, W.B. 1989. *The Architecture of Ancient Greece*. London: B.T. Batsford Limited.
- Doğer, E. 2006. Aigai'de Bir Macellum? *Miko, Ege Kültürü Dergisi*. 5.
- Doğer, E. 2007. Aigai 2004-2006 Yılı Kazıları. 29. Kazı Sonuçları Toplantısı I, 28 May- 01 June 2007. Kocaeli.
- Fichter, L.S., Farmer, G.T.Jr. 1975. *Earth Materials and Earth Process: An Introduction, Second Edition*. Minnesota: Burgess Publishing Company.

- Fitzner, B., Heinrichs, K. 2001. Damage diagnosis on stone monuments - weathering forms, damage categories and damage indices.- In Prikryl, R. & Viles, H.A. (Edit.): *Abstracts to the International Conference "Stone weathering and atmospheric pollution network (SWAPNET)", May 7-11, 2001*. 45(1):12 – 13. Prague: Charles University.
- Fitzner, B. 2004. Documentation and Evaluation of Stone Damage on Monuments. *Proceedings of the 10th International Congress on Deterioration and Conservation of Stone, June 27 - July 2, 2004*. ed. Kwiatkowski, D. and Löfvendahl, R. Sweden: ICOMOS.
- Friedman, I., Long, W. 1976. Hydration rate of obsidian. *Science* 191 (4225): 347-352.
- Frothingham, A.L.Jr. 1886. *The American Journal of Archaeology and of the History of the Fine Arts*. 2. 2 USA: Archaeological Institute of America.
- Gadsden, J.S. 1975. *Infrared Spectra of Minerals and Related Compounds*. London: Butterworths.
- Garrels, R.M. 1951. *A Textbook of Geology*. New York: Harper&Brothers.
- Herodotos 1991. *Herodot Tarihi*. I 149. Translated by M. Ökmen. İstanbul: Remzi Kitabevi.
- Howe, J.E. 2001. *The Geology of Building Stones*. USA: Donhead Publishind Ltd.
- ICOMOS Charter 2009. Charter for the Protection and Management of the Archaeological Heritage. [http://www.international.icomos.org/e\\_archae.htm](http://www.international.icomos.org/e_archae.htm) (accessed May 22, 2009).
- Iijima, K., Jiménez-Espejo, F., Sakamoto, T. 2004. "Filtration method" for semi-quantitative powder X-ray diffraction analysis of clay minerals in marine sediments. IFREE Report for 2003-2004. *Frontier Research on Earth Evolution 2*, [http://www.jamstec.go.jp/ifree/jp/05result/IFREE\\_Report\\_for\\_2003-2004/honbun/contents.pdf](http://www.jamstec.go.jp/ifree/jp/05result/IFREE_Report_for_2003-2004/honbun/contents.pdf).
- İpekoğlu, B., Böke, H., Çizer, Ö. 2007. Assessment of material use in relation to climate in historical buildings. *Building and Environment* 42 (2): 970-978.
- Lee, C.H., Yi, J.E. 2006. Weathering damage evaluation of rock properties in the Bunhwangsa temple stone pagoda, Gyeongju, Republic of Korea. *Springer-Verlag* 52 (6): 1193-1205.
- Monroe, J.S., Wicander, R. 2007. *Fiziksel Jeoloji, Yeryuvarı'nın Araştırılması*. translated by Dirik, K., Şener, M. İstanbul: Berkay Ofset Ltd. Şti.
- Oguchi, T.C., Matsukura, Y. 1999. Effect of porosity on the increase in weathering-rind thickness of andesite gravel. *Engineering Geology* 55(1-2): 77-89.

- Oguchi, T.C. 2001. Formation of weathering rinds on andesite. *Earth Surface Processes and Landforms* 26: 847-858.
- Oxley, T.A., Gobert, E.G. 1985. *The professionals and home owners guide to dampness in buildings: diagnosis treatment instruments*. London: Butterworths.
- Pansu, M., Gaytheyrou, J. 2006. *Handbook of Soil Analysis – Mineralogical, Organic and Inorganic Methods*. Berlin Heidelberg Netherlands: Springer-Verlag.
- Press, F., Siever, R. 2002. *Understanding Earth, Third Edition*. New York: W.H. Freeman and Company.
- RILEM 1980. Tests Defining the Structure. *Materials and Construction* 13 (73): 179-181.
- Roma Tre University 2008.  
[http://host.uniroma3.it/dipartimenti/mondo\\_antico/temnos/images/coast.jpg](http://host.uniroma3.it/dipartimenti/mondo_antico/temnos/images/coast.jpg)  
 (accessed June 2, 2008).
- Schaffer, R.J. 1932. *The Weathering of Natural Building Stones, Special Report No.18*. Garston, Watford: Building Research Establishment.
- Scherer, G.W. 2006. Internal Stress and Cracking in Stone and Masonry. In *Measuring, Monitoring and Modeling Concrete Properties*, ed. Konsta-Gdoutos, 633-641. Netherlands: Springer.
- Schiavon, N. 2006. Kaolinisation of granite in an urban environment. *Environmental Geology* 52: 399-407.
- Spock, L.E. 1953. *Guide to the Study of Rocks*. New York: Harper&Row Publishers.
- Tacitus 2009. *The Annals by Tacitus. Book 2*. Translated by Church, A.J. and Brodribb, W.J.  
<http://classics.mit.edu/Tacitus/annals.2.ii.html> (accessed January 23, 2009).
- Teutonico, J.M. 1988. Porous Building Materials. In *A Laboratory Manual for Architectural Conservators*, 35-68. Rome: ICCROM Publishing.
- Tokmak, M. 2005. Documentation and Examination of Historic Building Materials for the Purpose of Conservation: Case Study, Part of the Walls at the Citadel of Ankara. Master Thesis, Middle East Technical University, Ankara.
- Tuğrul, A. 1995. The effects of weathering on the engineering properties of basalts in the Niksar region. PhD Thesis. İstanbul University, İstanbul.
- Wycherley, R.E. 1993. Antik Çağda Kentler Nasıl Kuruldu? Translated by Nirven, N. and Başgelen, N. İstanbul: Arkeoloji ve Sanat Yayınları.